



**AgEcon** SEARCH  
RESEARCH IN AGRICULTURAL & APPLIED ECONOMICS

*The World's Largest Open Access Agricultural & Applied Economics Digital Library*

**This document is discoverable and free to researchers across the globe due to the work of AgEcon Search.**

**Help ensure our sustainability.**

Give to AgEcon Search

AgEcon Search

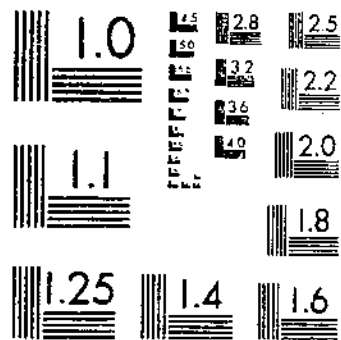
<http://ageconsearch.umn.edu>

[aesearch@umn.edu](mailto:aesearch@umn.edu)

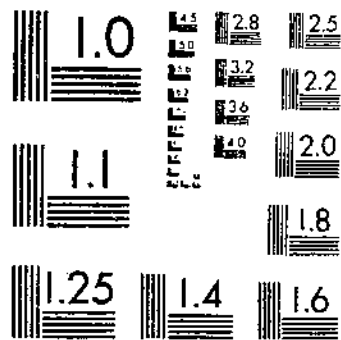
*Papers downloaded from **AgEcon Search** may be used for non-commercial purposes and personal study only. No other use, including posting to another Internet site, is permitted without permission from the copyright owner (not AgEcon Search), or as allowed under the provisions of Fair Use, U.S. Copyright Act, Title 17 U.S.C.*

TB 1466 (1973) USDA TECHNICAL BULLETINS SUPDATA  
STRUCTURAL DESIGN PROCEDURE FOR CORRUGATED PLASTIC DRAINAGE TUBING  
FOUSS, J L 1 OF 1

# START



MICROCOPY RESOLUTION TEST CHART  
NATIONAL BUREAU OF STANDARDS-1953-A



MICROCOPY RESOLUTION TEST CHART  
NATIONAL BUREAU OF STANDARDS-1963-A

R  
630

57

3-1

# STRUCTURAL DESIGN PROCEDURE FOR CORRUGATED PLASTIC DRAINAGE TUBING

Technical Bulletin No. 1466

3-1  
1975

Agricultural Research Service  
U.S. DEPARTMENT OF AGRICULTURE

in cooperation with  
The Ohio Agricultural Research and Development Center  
and  
Department of Agricultural Engineering  
Ohio State University

JUL 28 1976

JUL 23 1976

## ACKNOWLEDGMENTS

The author wishes to express appreciation to many colleagues for suggestions and assistance given in the preparation of this technical report—G. O. Schwab, N. R. Fausey, and B. H. Nolte, for reviewing and offering comments on the report; to R. C. Reeve, research investigations leader, who reviewed the report in depth and made detailed suggestions for improving it; and to Dennis L. Bassett, research assistant, who drafted all the figures and graphs in the report.

## CONTENTS

	Page
List of symbols .....	iv
Abstract .....	1
Introduction .....	1
Purpose and scope of the report .....	2
Flexible conduit principle .....	2
Design procedure .....	2
Principle .....	2
Step 1: General requirements and assumptions .....	3
Step 2: Design soil load .....	4
Step 3: Soil-conduit deflection .....	4
Step 4: Parallel-plate design load .....	6
Step 5: Plastic material specifications .....	6
Step 6: Moment-of-inertia of pipe wall .....	7
Step 7: Corrugation profile design .....	7
Step 8: Approximating minimum coiling radius for draintube .....	23
Step 9: Water-entry openings in draintube wall .....	24
Comments and discussion .....	26
Selected references .....	27
Appendix I .....	28
Appendix II .....	30
Analysis example 1 .....	30
Analysis example 2 .....	35
Appendix III .....	40

## LIST OF SYMBOLS

<i>Symbol or variable</i>	<i>Definition or description</i>	<i>Unit of measurement</i>
$A_s$	Shear area for one web over a quadrant of the tube circumference at the neutral axis ( <i>NA</i> ).	in. <sup>2</sup>
$A_{tw}$	Tube-wall circumferential area per unit length of tube.	in. <sup>2</sup> /lin. ft.
$A_w$	Cross-sectional area of tubing's corrugated wall per unit length of tube (one side only).	in. <sup>2</sup> /lin. ft.
$B_c$	Outside diameter (OD) of draintube.	ft.
$C$	Distance from <i>NA</i> to outer or innermost tube wall fiber.	in.
$C'$	Maximum distance from <i>NA</i> to outer or innermost tube wall fiber.	in.
$C_c$	Soil load concentration factor related to $(H_s/B_c)$ ratio and soil type.	
$C_{R_{min}}$	Minimum inside radius at which tubing can be coiled.	in.
$c$	Proportionality constant between outside and inside wall thickness ( $T_o \Delta c T_i$ ).	
$D_i$	Inside diameter (ID) of draintube.	in.
$D_l$	Deflection lag factor (generally between 1.0 and 1.5).	
$D_{NA}$	Diameter of tube to the neutral axis ( <i>NA</i> ) of the tube-wall cross section.	in.
$D_o$	Outside diameter (OD) of draintube.	in.
$E$	Modulus of elasticity (Young's Modulus) for the tube-wall material.	p.s.i.
$E'$	Soil modulus term.	p.s.i.
$E_{design}$	Design value for the plastic material modulus of elasticity.	p.s.i.
$(EI)$	Section modulus of tube wall.	$\frac{\text{lb.}\cdot\text{in.}^2}{\text{lin. in.}}$
$EI_r$	Required section modulus for tube wall.	$\frac{\text{lb.}\cdot\text{in.}^2}{\text{lin. in.}}$
$\left[ \frac{EI}{D_{NA}^3} \right]$	Conduit stiffness factor.	lb./in. <sup>2</sup>
$H$	Effective structural depth of corrugations.	in.
$H'$	One-half the difference between the ID and OD of the tube (overall depth of corrugation).	in.
$H_s$	Depth of soil to top of drain.	ft.
$h$	Physical depth of corrugation.	in.
$h'$	Maximum lateral soil pressure at the side of conduit.	p.s.i.
$I$	Moment-of-inertia of the tube-wall cross section, per unit of tube length.	in. <sup>4</sup> /lin. in.
$I_r$	Required moment-of-inertia for tube wall.	in. <sup>4</sup> /lin. in.
$K_S$	Bedding factor constant related to conduit bedding angle.	
$k$	Distance from <i>NA</i> of the corrugation profile to the centerline of the horizontal thickness of the corrugation ridge.	in.
$\mathcal{C}$	Centerline.	
$L_i$	Length of corrugation root at inside diameter.	in.
$L_o$	Length of corrugation ridge at outside diameter.	in.
$M$	Bending moment in the tube wall per unit length of tube.	$\frac{\text{in. lb.}}{\text{lin. in.}}$
$NA$	Neutral axis of the corrugated tube-wall cross section.	
$P$	Corrugation pitch.	in.

Symbol or variable	Definition or description	Unit of measurement
$R_C$	Radius of curvature for centerline of the tubing when coiled.	in.
$R_i$	Inside radius of coil of tubing.	in.
$S$	Total shear force around one quadrant of one corrugation web.	lb.
$T$	Tube-wall thickness (if constant).	in.
$T_i$	Thickness of tube wall at the inside diameter.	in.
$T_o$	Thickness of tube wall at the outside diameter.	in.
$T_w$	Thickness of tube wall webs.	in.
$v$	Volume of plastic material per unit length of drain tubing.	in. <sup>3</sup> /lin. in.
$v_p$	Measured volume of plastic tube specimen.	cm. <sup>3</sup>
$W$	Parallel-plate load applied, per unit tube length.	lb./lin. ft.
$W_c$	Total soil load on conduit, per unit tube length.	lb./lin. ft.
$w$	Tubing unit weight.	lb./lin. ft.
$w_e$	Unit soil load on conduit.	p.s.i.
$w_s$	Unit weight of soil.	lb./ft. <sup>3</sup>
$2\alpha$	Soil bedding angle under tubing.	deg.
$\gamma_{H_2O}$	Density of water.	lb./in. <sup>3</sup>
$\gamma_p$	Density of plastic in tube specimen.	g./cm. <sup>3</sup>
$\Delta x$	Change in horizontal tube diameter.	in.
$\Delta x_{design}$	Design value of horizontal tube deflection.	in.
$\Delta x_{pl}$	Change in horizontal diameter when maximum total tube-wall stress is at the proportional limit.	in.
$\frac{\Delta x_{pl}}{w}$	Plastic-use-efficiency factor.	in.-lb. lin. ft.
$\Delta x_s$	Change in horizontal diameter of draintube under soil loading.	in.
$\Delta y$	Change in vertical tube dia.	in.
$\delta$	For angled web corrugation profiles, the longitudinal distance between adjacent ends of the ridge ( $L_o$ ) and root ( $L_i$ ).	in.
$\epsilon_{pl}$	Proportional limit of strain.	in./in.
$\theta$	Angle between corrugations for coiled tubing.	rad.
$\rho_p$	Specific gravity of plastic material.	
$\sigma_B$	Bending stress in tube wall.	p.s.i.
$\sigma_{BC}$	Compressive component of tube wall bending stress.	p.s.i.
$\sigma_{BT}$	Tensile component of tube wall bending stress.	p.s.i.
$\sigma_{Bpl}$	Bending stress component when maximum total stress in tube wall is at the proportional limit.	p.s.i.
$\sigma_c$	Pure ring-compression stress in tube wall.	p.s.i.
$\sigma_{pl}$	Proportional limit of stress.	p.s.i.
$\sigma_S$	Shear stress in corrugation webs.	p.s.i.
$\sigma_{TC}$	Maximum total tube wall stress (in compression).	p.s.i.
$\sigma_{TT}$	Total net stress in the tube wall (in tension).	p.s.i.
$\sigma_{YP}$	Yield point stress for plastic material.	p.s.i.
$\Phi$	Web angle related to contraction of corrugation pitch on the inner tube coiling radius.	rad.
$\frac{\Delta}{\alpha}$	Is defined as . Proportional to.	

# STRUCTURAL DESIGN PROCEDURE FOR CORRUGATED PLASTIC DRAINAGE TUBING

By JAMES L. FOUSS, *agricultural engineer, Southern Region, Agricultural Research Service, United States Department of Agriculture, Florence, S.C.*

## ABSTRACT

This report presents a systematic, analytical procedure for design selection of a structurally efficient corrugation shape for the wall of plastic drainage tubing. The design objective is to maximize the tube strength-to-tube weight ratio within the bounds of allowable tube-wall stress and strain. Although the design procedure establishes the requirements for draitube strength and deflection in terms of soil loads, the design analysis and selection technique simplify the engineering evaluation of various corrugation profiles by the use of equivalent parallel-plate load and deflection parameter of the draitube.

Throughout the report, all equation derivations needed for the design analysis and computations are given in detail. The more important equations point out general proportional relations between tube strength ( $W$ ) [for a constant deflection ( $\Delta x$ )], and plastic thickness ( $T$ ), corrugation depth ( $H$ ), corrugation pitch ( $P$ ), and tube weight ( $w$ ): such as  $W \propto T$ ;  $W \propto H^3$ ;  $W \propto 1/P$ ; and  $W \propto w$ . The equations used and the outline of computational techniques are illustrated by a complete design example for 4-inch diameter, corrugated plastic drain tubing. In addition, two analysis examples for sample corrugated plastic draitubes illustrate the accuracy of the design procedure.

A testing procedure is outlined and an example is given for determining the physical properties of the particular plastic material to be used in fabricating drain tubing. For example, the modulus of elasticity ( $E$ ) can be evaluated from stress-strain tests conducted at a very *low* strain-rate. Published values of ( $E$ ), determined in accordance with some American Society for Testing Materials (ASTM) procedures, are shown to be too high and are, therefore, not appropriate for use in the design analysis outlined.

Appropriate graphs, showing the numerical results for the design example, illustrate the *combined* effects of the various corrugation profile dimensions on tube strength and weight—such as plastic thickness ( $T$ ), depth of corrugations ( $H$ ), and corrugation pitch ( $P$ ). When the corrugation design is finally selected, the importance of various practical considerations are spelled out. The significance of typical soil-loading cycles on the drain tubing and the factor-of-safety provided by recoverable strain in the plastic material are discussed.

An analytical method is presented for approximating the minimum coiling radius of drain tubing for a given corrugation profile. General guidelines are given for the design and location of openings in the tube wall for water entry.

## INTRODUCTION

New materials for subsurface soil drainage have been developed in more than 20 years of research. Of these materials, corrugated-wall, plastic drain tubing is rapidly being accepted for use on farms in the United States, Canada, and Europe.<sup>1</sup> The corrugated plastic tubing is flexible (coilable), light weight, and easier to install than clay or concrete draitile and rigid plastic drainpipe in specified lengths. Also, flexible plastic drainage tubing can be rapidly plowed into the ground with the newly developed draitube plow equipment,<sup>1</sup> thus eliminating the time-consuming and costly ditching and backfilling operations that are common today for installing drains.

As with most new materials, some disadvantages of flexible plastic tubing will require the development of new methods for its use and maintenance. For instance, for the same nominal size drain, the corrugated-wall tube has less hydraulic capacity

<sup>1</sup> See Selected References on p. 27 for additional reading material on this subject.



because of loss by friction than the smooth-walled tube. Care must be taken not to stretch the corrugated-wall tubing during installation. Once installed, the plastic drain tubes cannot be located with the conventional tile probe without risk of puncturing the tube walls. Also, many plastic drain materials may be damaged by excessive heat or fire.

When compared with smooth-wall plastic tubing, the corrugated-wall tubing provides greater strength, may be coiled without kinking, is lighter weight, and is much lower in cost. To be of equal structural strength, a smooth-wall plastic tube of a given diameter must be much thicker than a corrugated-wall tube of the same diameter; therefore, the smooth-wall tubing would be considerably heavier. Since the cost of plastic tubing is essentially proportional to its weight per linear foot for tubes of equal strength, smooth-wall tubing typically costs four to six times more than corrugated tubing.

The corrugated plastic drainage tubing commercially available (1970) in the United States and Europe is generally acceptable, in terms of structural strength and cost, for use in agricultural drainage. However, because of the corrugation shapes used in some of the production tubes, the plastic material in the tube walls is not used efficiently. By applying basic engineering design principles, an engineer can use the plastic material more efficiently and plastic drain tubing can be produced at still lower cost.

## PURPOSE AND SCOPE OF THE REPORT

This report presents a systematic, analytical procedure for designing an efficient corrugation shape (cross section) for the wall of the plastic draitube. Each step of the procedure is discussed in considerable detail. In principle, this design method follows very closely the procedure used for the optimized design of a structural I-beam; that is, within the confines of practical dimensions, the cross section is designed to obtain maximum moment-of-inertia in the tube wall with a maximum strength-to-weight ratio for the fabricated plastic tube.

The report does not deal with the hydraulic aspects of the draitube design, except as tube-wall perforations (or slots for water entry) affect the structural strength and design efficiency.

Although English units are used throughout the main text of the report, the major equations used in conducting a design analysis and the definitions of terms are given in metric units in Appendix III.

## FLEXIBLE CONDUIT PRINCIPLE

A corrugated plastic draitube is a flexible conduit. The flexible tube, when installed, gains part of its vertical soil load-carrying capacity by lateral support (passive resistance)<sup>2</sup> from the soil surrounding the sides of the draitube. This lateral support occurs as the draitube flattens and deflects outward against the soil at its sides. The phenomenon is often referred to as a soil-conduit interaction. When this interaction is considered in flexible conduit design, plastic material, which is expensive, is used more efficiently. The tube's resistance to bending stress does not come entirely from the tube walls as it does in rigid conduits.

## DESIGN PROCEDURE

### Principle

The design principle followed here involves the use of the strength-deflection characteristic of the flexible conduit under parallel-plate loading (that is, top and bottom concentrated loads). This concept is used as a matter of convenience and is illustrated in step 4 of the analysis. It is applicable when a design is formulated for a new flexible conduit and when structural analysis is made of an existing conduit.

Figure 1 shows in schematic the parallel-plate, load-deflection method of testing a flexible draitube sample. For plastic draitube design evaluation purposes, the following test procedure is recommended. The parallel-plate load ( $W$ ) should be applied accumulatively in increments, such that incremental changes in vertical tube deflection ( $\Delta y$ ) do not exceed about 0.5 percent of  $D_{NA}$ , when the deflection is measured (recorded) at time intervals of 1 to 3 minutes after each load increment is added. This slowly applied incremental loading permits sufficient time for most of the creep

<sup>2</sup> Passive resistance is defined as the pressure that results when the tubing wall moves toward and against the soil; active resistance is the pressure that results when the soil moves toward and bears against the tube wall.

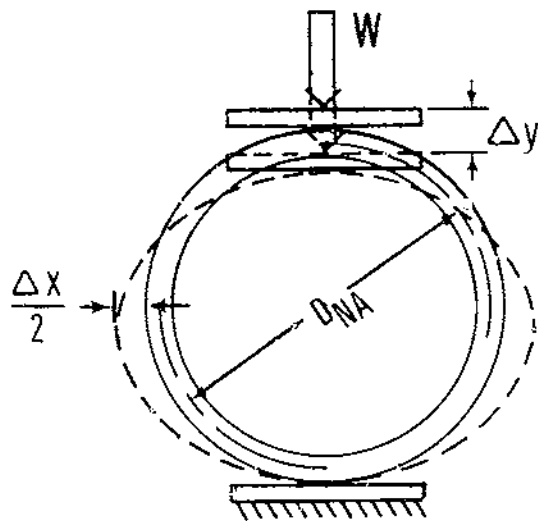
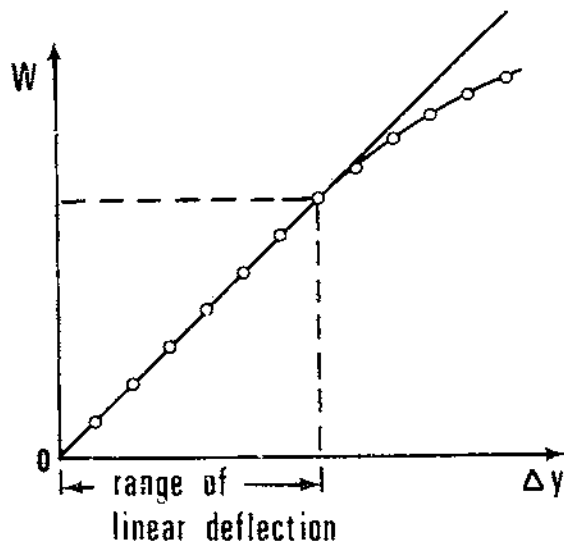


Figure 1.— Parallel-plate, load-deflection method of testing flexible (plastic) drainage tubing.



strain, if any, to occur for tube deflection within the linear range. From the theory of strength of elastic materials (many plastic materials are elastic for small deflection or strain), the vertical, horizontal, or both, conduit diameter changes (deflection  $\Delta y$  and  $\Delta x$ , respectively), up to the linear deflection limit, can be related to the applied concentrated load ( $W$ ) by the following theoretical equations (3, 21):<sup>3</sup>

$$\Delta y = 0.1488 \frac{\left(\frac{D_{NA}}{2}\right)^3}{EI} \left(\frac{W}{12}\right) \quad [1]$$

$$\Delta x = 0.1366 \frac{\left(\frac{D_{NA}}{2}\right)^3}{EI} \left(\frac{W}{12}\right) \quad [2]$$

where,

- $\Delta y$   $\triangleq$  change in vertical tube diameter (in.);
- $\Delta x$   $\triangleq$  change in horizontal tube diameter (in.);
- $D_{NA}$   $\triangleq$  diameter of tube to the neutral axis (NA) of the tube-wall cross section (in.);
- $E$   $\triangleq$  Modulus of elasticity (Young's Modulus) for tube-wall material (p.s.i.);

$I$   $\triangleq$  moment-of-inertia of the tube-wall cross section per unit tube length (in.<sup>4</sup>/lin. in.);

$W$   $\triangleq$  parallel-plate load applied (lb./lin. ft.); 0.1488 and 0.1366 are dimensionless constants related to angular position around the circumference;

2 = the dimensionless ratio between tube diameter and radius;

12 = conversion constant (in./ft.).

Note: The product  $(EI)$   $\triangleq$  section modulus of tube wall,  $\left(\frac{\text{lb.}\cdot\text{in.}^2}{\text{lin. in.}}\right)$ ; and term  $\left[\frac{EI}{D_{NA}^3}\right]$   $\triangleq$  conduit stiffness factor (lb./in.<sup>2</sup>).

Equations 1, 2, or both can be used to theoretically predict the deflection of a given conduit under some known parallel-plate load. More importantly, the equations can be used as design equations, illustrated by the following example of design analysis.

### Step 1: General Requirements and Assumptions

For this example design analysis, a corrugation shape for a drain tube with 4-inch inside diameter is considered. The drain tube is to be installed at a

<sup>3</sup> Italic numbers in parentheses refer to Selected References, p. 27.

depth of 4 to 6 feet in a 2-foot wide trench. The soil is assumed to be saturated clay. The loads imposed under such conditions are considered to be maximum, which is needed information for design purposes.

The effect of surface loads over the drainpipe is neglected. Generally, additional loads caused by surface traffic are small (4, 12) where drains are more than 3 feet deep.

### Step 2: Design Soil Load

To approximate the design soil load for the conditions previously stated, the classical procedures for computing loads on buried conduits are used (12). Because of the wide trench and small-diameter tube, the "projecting ditch condition" applies and the soil load is computed by using the equation

$$W_c = C_c w_s B_c^2 \quad [3]$$

where,

$W_c$   $\triangleq$  total soil load on conduit, (lb./lin. ft.);  
 $C_c$   $\triangleq$  load concentration factor related to  $\left(\frac{H_s}{B_c}\right)$  ratio and soil type, where  $H_s$   $\triangleq$  drain depth, (ft.), (This factor can be determined graphically from (12, fig. 18.7, p. 475);

$w_s$   $\triangleq$  unit weight of soil, (lb./ft.<sup>3</sup>);

$B_c$   $\triangleq$  outside diameter of draintube, (ft.).

In the analysis the assumption is;

A positive settlement ratio in the ditch back-fill (21)

$w_s = 120$  lb./ft.<sup>3</sup> (for saturated clay)

$B_c = \frac{4.5 \text{ in.}}{12 \text{ in./ft.}} = 0.375$  ft. (for inside tube dimension of 4 in.)

$H_s = 6$  ft. (maximum installation depth),

then,  $\frac{H_s}{B_c} = \frac{6.0}{0.375} = 16$ ;  $C_c \approx 29$  (by interpolation from (12, fig. 18.7, p. 475)).

So,  $W_c \approx (29)(120)(0.375)^2 = 489$  lb./lin. ft.

Therefore,  $W_c = 500$  lb./lin. ft. becomes the design soil load.

The conduit load will not be multiplied by the usual factor-of-safety. As the draintube deflects slightly under the soil loading, forces change within the soil around the tubing, and soil pressure relaxes on the top half of the tubing. This phenomenon is

commonly referred to as "bridging" or "arching." Thus, the flexible nature of the tubing creates a built-in factor-of-safety. In addition, this design load is a maximum which occurs when the soil is saturated. Experiments have shown that the soil load on the conduit varies with the wetting and drying cycles. In fact, as a clay soil surrounding the draintube or conduit becomes very dry, even during a short-term drought, the soil shrinks away from the tube walls; thus, no load is imposed on the draintube. The cyclic nature of the soil load is important when creep-strain in the plastic material of the tube walls is considered. This is discussed in more detail in step 5 of the analysis.

### Step 3: Soil-Conduit Deflection

The required section modulus ( $EI$ ) of the tube wall is determined next and will limit the conduit deflection ( $\Delta x$ ) to an allowable percentage of the tube diameter for the design load. The revised Iowa Formula, developed by Watkins and Spangler (23) can be used to calculate ( $EI$ ) as shown below. Spangler's original derivation of the formula for predicting deflection of buried flexible pipe or tubing was based on the assumed soil load and passive reaction shown in figure 2. The revised Iowa Formula is the form shown below for use herein:

$$\Delta x_s = \frac{D_i K_S \left(\frac{W_c}{12}\right) \left(\frac{D_{NA}}{2}\right)^3}{EI + 0.061 E' \left(\frac{D_{NA}}{2}\right)^3} \quad [4]$$

where,

$\Delta x_s$   $\triangleq$  change in horizontal diameter of draintube under soil loading, (in.);

$D_i$   $\triangleq$  deflection lag factor (generally between 1.0 and 1.5);

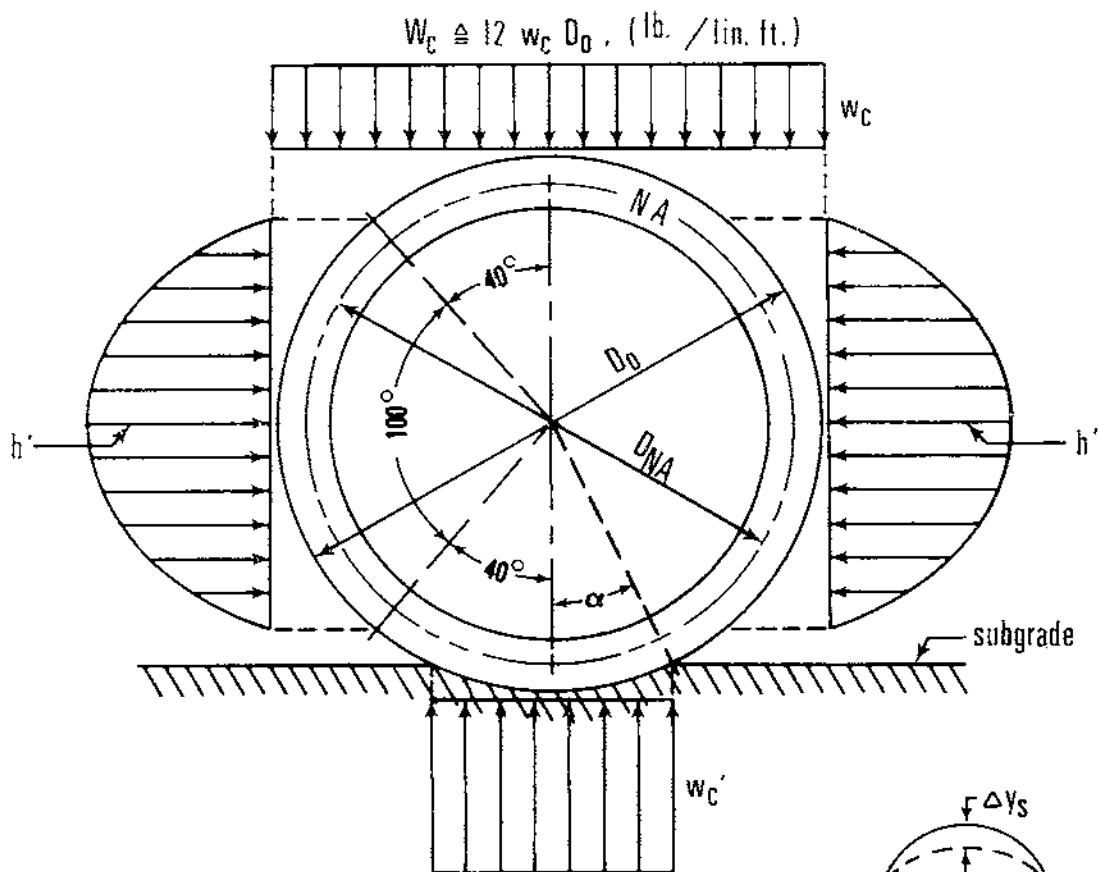
$K_S$   $\triangleq$  Bedding factor constant related to conduit bedding angle (see fig. 2);

$E'$   $\triangleq$  Soil modulus term (p.s.i.). (Typical values for various soils are: Sand—2,000 to 3,000 p.s.i.; wet clay—600 to 800 p.s.i.; and saturated clay—less than or equal to 600 p.s.i.)

0.061 = a dimensionless constant, and,

$W_c$ ,  $D_{NA}$ ,  $E$ , and  $I$  as defined previously.

When equation 4 is solved for the product term ( $EI$ ) that is,



where,  $\frac{h}{(\Delta x_s / D_{NA})} \cong E'$ , Soil modulus

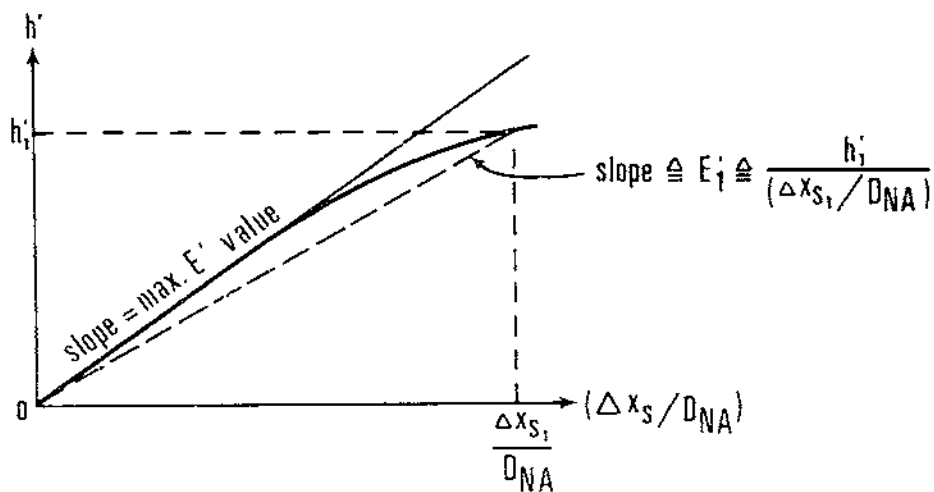


Figure 2. — Assumed soil-loading distribution and passive soil reaction for derivation of Iowa Formula (23).

$$EI = \frac{D_i K_s \left( \frac{W_c}{12} \right) \left( \frac{D_{NA}}{2} \right)^3}{\Delta x_s} - 0.061 E' \left( \frac{D_{NA}}{2} \right)^3, \quad [5]$$

and substituted in the following specified values for the equation parameters which are commensurate with this example, the required value for ( $EI$ ) is obtained.

$D_L = 1.0$  (select allowable short-term deflection  $\Delta x_s$  accordingly);

$K_S = 0.110$  (for flat bottom ditch; table of values given in (21));

$W_c = 500$  lb./lin. ft. (from step 2);

and,

$D_{NA} = 4.25$  in. (this should provide a tube with an inside diameter ( $D_i$ )  $\approx 4.0$  in.);

$E' = 400$  p.s.i.;

$\Delta x_s = 0.17$  in., i.e., 4 percent of  $D_{NA}$  is assumed.\*

Thus, by equation 5 the required section modulus ( $EI_r$ ) for the tube wall is:

$$EI_r = 24.6 \frac{\text{lb. in.}^2}{\text{lin. in.}}$$

#### Step 4: Parallel-Plate Design Load

This step is one of convenience in design as indicated under design principle. The object is to compute and use the equivalent parallel-plate load ( $W$ ) which will cause the same conduit deflection as that caused by the design soil load ( $W_c$ ). That is, for

$\Delta x = \Delta x_s = 0.17$  in., or 4 percent of  $D_{NA} = 4.25$  in., and

$$EI = 24.6 \frac{\text{lb. in.}^2}{\text{lin. in.}},$$

from equation 2,

$$W = 38.4 \text{ lb./ft. @ } \Delta x = 0.17 \text{ in.}$$

The parallel-plate, load-deflection characteristic is expressed more conveniently in terms of vertical deflection ( $\Delta y$ ). In fact, this characteristic is the easier to measure when testing a tube specimen as shown schematically in figure 1. Therefore, to

express this parallel-plate design load ( $W$ ) in terms of ( $\Delta y$ ), equations 1 and 2 can be solved to express  $\Delta y = f(\Delta x)$ ; that is,

$$\Delta y = \frac{0.1488}{0.1366} \Delta x = (1.09) \Delta x \quad [6]$$

So for  $\Delta x = 0.17$  in.  $\Rightarrow \Delta y = (1.09) (0.17) = 0.185$  in. ( $\approx 4.35$  percent of  $D_{NA}$ ). Thus, the equivalent parallel-plate design load can be written as

$$W = 38.4 \text{ lb./ft. @ } \Delta y = 0.185 \text{ in.}$$

between parallel plates.

In the following sections, a proposed corrugation design is evaluated in terms of the parallel-plate, load-deflection resistance that the design provides for the tube, and then the tube's strength is compared with the design load computed in this analysis step.

#### Step 5: Plastic Material Specifications

The following plastic material is considered in this design example: High density polyethylene (HDPE), Type III, Class C, Category 3, as specified in ASTM Designation D 1248-69. This is the most common plastic material used in the United States through 1970, for fabricating corrugated plastic drainage tubing. Polyvinyl-chloride (PVC) plastic has been more commonly used in Europe. Only a brief comparison and discussion of these two types of plastic is given here. HDPE has better impact resistance than PVC, especially at temperatures near 0° C., but PVC is much stronger and more rigid than HDPE. For example,  $E_{PVC} \approx 3 E_{HDPE}$ , but the types of corrugated tubing extrusion equipment in use during 1970 has not made it possible to fabricate PVC tubing with walls thin enough to fully and efficiently utilize the higher strength PVC material. Thus, the current use of HDPE results in lower cost tubing. While PVC is superior to HDPE in creep-strain resistance, HDPE is suitable for fabricating the drainage tubing (10). In step 2, it was pointed out that, with the soil wetting and drying, the soil load on the tube is cyclic. For most conditions, any creep strain that occurs in the tube wall (if such strain is less than the yield-point strain) during a prolonged wet cycle can relax during a subsequent dry period. Forming a supporting groove (cradle) in the bottom of the trench is

\* The linear deflection range predictable by the Iowa Formula is generally considered to be  $\Delta x_s \leq 5$  percent of  $D_{NA}$ ; see (21 and 23).

recommended, when the tubing is installed (22), so as to support the bottom half of the tube circumference. This added margin-of-safety will prevent HDPE plastic tubes from being overly deflected by the initial wetting and settlement of the soil backfill in the trench.

Structurally, the modulus of elasticity ( $E$ ) of the plastic material is one of the more important mechanical properties of the corrugated plastic draintube. Equations 1 and 2 show that strength of the draintube (expressed in terms of load-deflection ratio) varies directly with  $E$ ; that is,

$$\frac{W}{\Delta y} = \left[ \frac{12I}{0.1488 \left( \frac{D_{NA}}{2} \right)^3} \right] \cdot E \quad [7]$$

where,

$$\left[ \frac{12I}{0.1488 \left( \frac{D_{NA}}{2} \right)^3} \right] = \text{a constant}$$

for any draintube of given diameter and corrugation shape. The actual value of ( $E$ ) for a particular HDPE plastic resin is governed primarily by the specific gravity ( $\rho_p$ ) and, to some degree, by melt index ( $MI$ ). For example, with  $\rho_p = 0.94$ , the corresponding modulus of elasticity is  $E \approx 50,000$  p.s.i., and at  $\rho_p = 0.96$ ,  $E \approx 140,000$  p.s.i. (1).

A strain rate of 2 in./min. was used to determine these  $E$ -values, in accordance with ASTM Test D 638. The strain rate may possibly be satisfactory for PVC but is considered too high for determining the  $E$ -value of HDPE plastic<sup>5</sup> for use in designing corrugated tubing as outlined in this report. Thus, one of the following alternatives should be used to determine a conservative  $E$ -value of the HDPE plastic for use in the design analysis:

1. Test a sample of the plastic in tension in accordance with ASTM Test D 638 but at a slower strain rate (e.g., 0.050 in./min.), or by incremental static loading, as shown in figure 3. For the incremental loading method, the following procedure is recommended: Apply the tensile force ( $F$ ) accumulatively in static weight increments ( $\Delta F$ ),

so that incremental changes in strain ( $\epsilon$ ) do not exceed about 0.2 percent when the distance ( $L + \Delta L$ ) between gage-length marks is measured with the cathetometer instrument at time intervals of 1 to 3 minutes after each ( $\Delta F$ ) increment is applied. (For example test run, see Appendix I.)

2. Test a specimen of smooth- or corrugated-wall tubing, made from the type of plastic resin of interest, in accordance with the parallel-plate, load-deflection method shown in figure 2. Calculate the  $E$ -value through use of equation 1 herein (for smooth-wall tubing,  $I = T^3/12$  in.  $\left( \frac{\text{in.}^4}{\text{lin. in.}} \right)$ , where  $T$  is tube-wall thickness; computation of ( $I$ ) for corrugated-wall tubing is covered in step 7a).

3. As a rule of thumb, set  $E_{\text{design}}$  at about one-half to two-thirds of the published  $E$ -value determined in accordance with ASTM Test D 638 when strain rate  $\cong 0.050$  in./min. is used.

In this design example, a sample of Type III, HDPE ( $\rho_p \approx 0.959$ ) was tested in accordance with the method illustrated in figure 3. Results of test data and computations for ( $E$ ) are presented in Appendix I—the resulting design value is

$$E_{\text{design}} = 95,000 \text{ p.s.i.},$$

with proportional (linear) limit of stress ( $\sigma_{pl}$ ) and strain ( $\epsilon_{pl}$ ) at about 1,000 p.s.i. and 1 percent, respectively. (By alternative method (3):  $2/3 \times 140,000 = 93,000$  p.s.i.)

### Step 6: Moment-of-Inertia of Pipe Wall

In step 3, the required value of  $EI_r = 24.6 \frac{\text{lb. in.}^2}{\text{lin. in.}}$  was determined, and in step 5 the design value of  $E = 95,000$  p.s.i. was selected; the required moment-of-inertia ( $I_r$ ) of the corrugated tube wall is now computed as:

$$I_r = \frac{EI_r}{E} = \frac{24.6 \frac{\text{lb. in.}^2}{\text{lin. in.}}}{95,000 \text{ lb./in.}^2} \quad [8]$$

or,

$$I_r = 0.000259 \frac{\text{in.}^4}{\text{lin. in.}}$$

### Step 7: Corrugation Profile Design

This design step proposes several corrugation profiles or shapes which will provide the required

<sup>5</sup> The strain rate of 2 in./min. may be satisfactory for more rigid plastic materials, such as PVC, where  $E_{PVC} \approx 300,000$  p.s.i.

moment-of-inertia (that is,  $I_r \approx 0.00026$  in.<sup>4</sup>/in.). The final corrugation design will be selected on the basis of plastic-use efficiency and tube-wall stress analysis. The corrugation profile to be considered in the example design problem is shown in figure 4(A), and the assumed structural equivalent profile is shown in figure 4(B).<sup>6</sup>

**7a: Equation for computing moment-of-inertia (I).**—The terminology shown in figure 4(B) is used to derive an equation that employs classical principles of engineering mechanics for computing the moment-of-inertia ( $I$ ) per linear inch of tubing:

$$I = \frac{1}{P} \left[ \underbrace{\frac{2T_w H^3}{12}}_{\text{for webs}} + \underbrace{\frac{L_i T_i^3}{12} + L_i T_i \left(\frac{H}{2}\right)^2}_{\text{for root}} \right. \\ \left. + \underbrace{\frac{L_o T_o^3}{12} + L_o T_o \left(\frac{H}{2}\right)^2}_{\text{for ridge}} \right] \quad [9]$$

which simplifies to:

$$I = \frac{1}{12P} [2T_w H^3 + L_i T_i^3 + L_o T_o^3 + 3H^2 (L_i T_i + L_o T_o)] \quad [10]$$

with units of (in.<sup>4</sup>/lin. in.); where,

$I$  Moment-of-inertia of the tube-wall cross section, per unit of tube length (in.<sup>4</sup>/lin. in.);

$P$  Corrugation pitch (in.);

$T$  Plastic material thickness, (in.); (subscripts  $w$ ,  $i$ , and  $o$  indicate web, inside (root), and outside (ridge) respectively);

$H$  Effective structural depth of corrugations (in.).

To reduce the number of individual variables needed for each trial corrugation profile, the following relationships are assumed (see fig. 4(B) for definition of terms):

<sup>6</sup>For this design example, a rather simple corrugation profile was selected to illustrate general analysis procedures. In practice, however, a more detailed analysis can be followed to account for large fillets, rounded sections, or both, that may be used in the corrugation profile. In fact, curved sections in the profile often improve extrusion and molding.

$$P = L_i + L_o \quad [11]$$

The neutral axis ( $NA$ ) of the corrugation profile should coincide with the centerline ( $\mathcal{E}$ ) of the profile<sup>7</sup> to equalize strain in the outer and inner plastic fibers of the tube wall, (that is, the ridge and root of the corrugation profile) as conduit deflection occurs; this condition exists, and  $NA \equiv \mathcal{E}$  if the following mathematical expression is satisfied:

$$T_i L_i \equiv T_o L_o \quad [12]$$

Thus, for this design example, the distance from the centerline of the ridge-wall thickness ( $T_o$ ) to the  $NA$  can be expressed as:  $k\Delta H/2$  (see fig. 4(B)). If the outside wall thickness ( $T_o$ ) is expressed as some proportion ( $c$ ) of the inside-wall thickness ( $T_i$ ), that is

$$T_o \Delta c T_i \quad [13]$$

then both  $L_o$  and  $L_i$  can be expressed in terms of  $P$ ; from equations 11, 12, and 13,

$$L_o = \frac{P}{(1+c)} \quad [14]$$

and

$$L_i = c L_o = \left( \frac{c}{1+c} \right) P \quad [15]$$

Furthermore, it may be assumed that

$$T_w \approx \frac{T_i + T_o}{2} \quad [16]$$

or by equation 13

$$T_w = \left( \frac{1+c}{2c} \right) T_o \quad [17]$$

Thus, equation 10 can now be modified if equations 13, 14, 15, and 17, are used so that only the variables  $c$ ,  $P$ ,  $H$ , and  $T_o$  need to be selected for a trial corrugation profile; that is,

<sup>7</sup>In general, the shift of the  $NA$  due to a curved-beam effect is negligible since the corrugation depth ( $H$ ) to tube radius ( $D_{NA}/2$ ) ratio is small.

<sup>8</sup>Experience based on present-day corrugated tubes indicates that a typical value for ( $c$ ) is  $\frac{3}{2}$ .

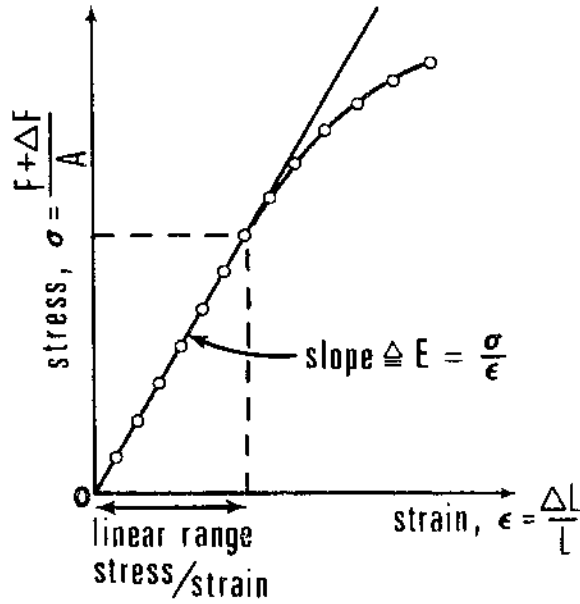
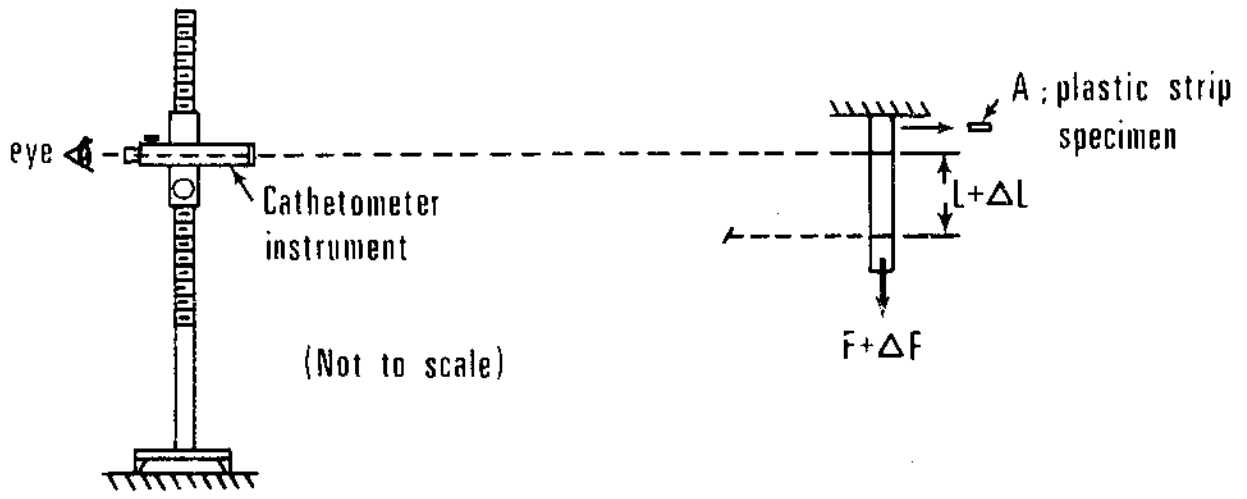


Figure 3. — Simplified method of stress-strain measurement to determine the modulus of elasticity ( $E$ ) for HDPE plastic material.



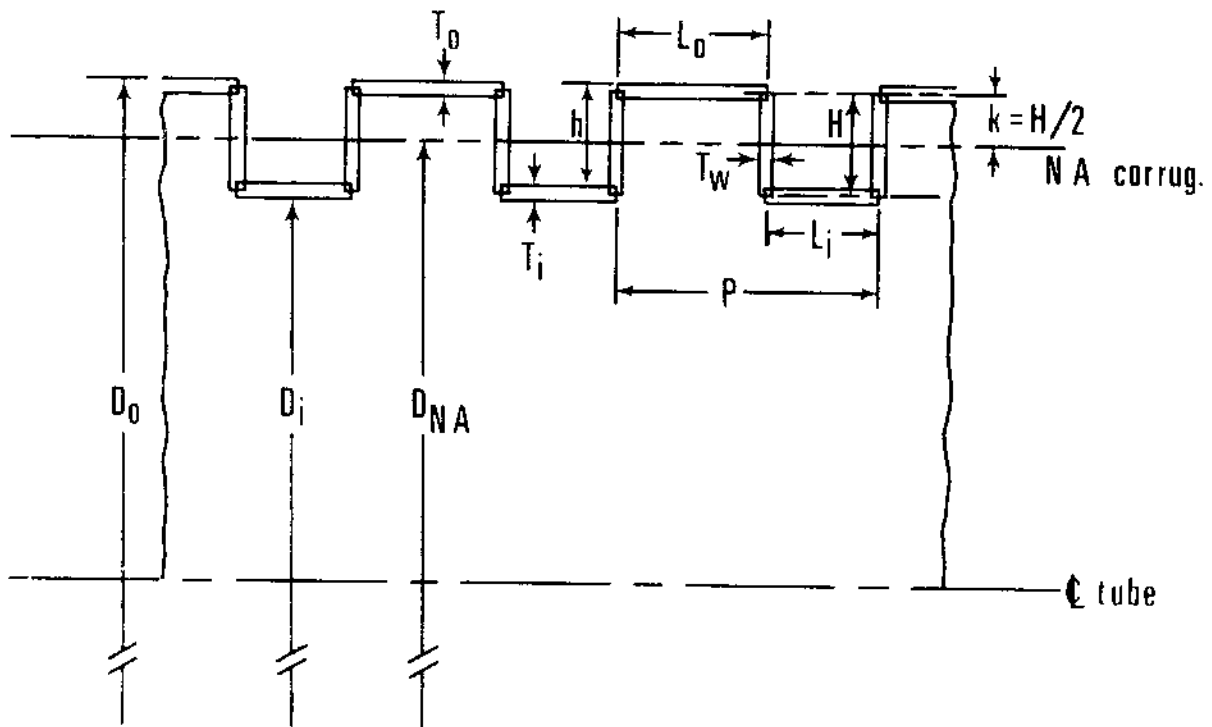
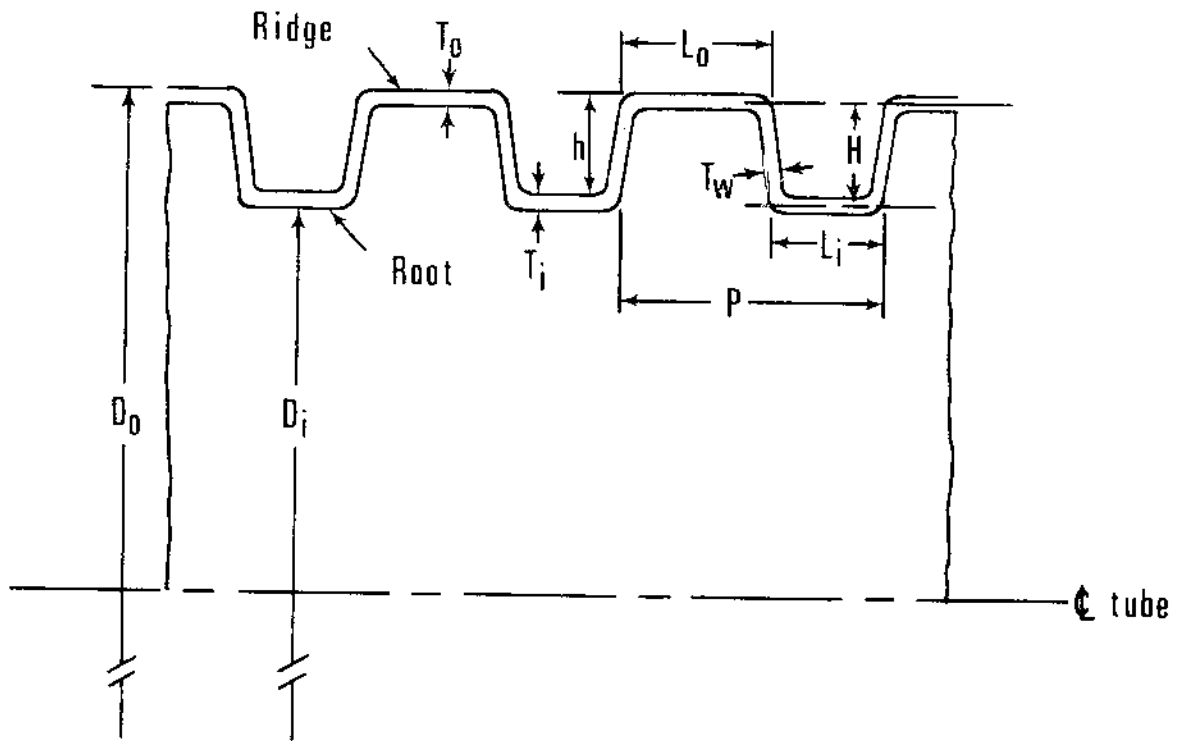


Figure 4. — General tube-wall corrugation profile, and definition of geometrical terms.

$$I = \frac{1}{12P} \left[ \left( \frac{1+c}{c} \right) T_o H^3 + \left( \frac{c}{1+c} \right) P \left( \frac{T_o}{c} \right)^3 \right. \\ \left. + \frac{P}{(1+c)} T_o^3 + 3H^2 \left( \frac{2P T_o}{1+c} \right) \right], \quad [18]$$

which simplifies to

$$I = \frac{1}{12} \left\{ \left[ \left( \frac{1+c}{c} \right) \frac{H^3}{P} + \left( \frac{6}{1+c} \right) H^2 \right] T_o \right. \\ \left. + \left[ \frac{1+c^2}{c^2(1+c)} \right] T_o^3 \right\} \quad [19]$$

For a specific value of ( $c$ ), however, the equation becomes a rather simple computational formula; that is, with  $c = 2/3$ , equation 19 becomes

$$I = \frac{1}{12} \left\{ \left[ (2.5) \frac{H^3}{P} + (3.6) H^2 \right] T_o + (1.95) T_o^3 \right\}; \quad [20]$$

(in<sup>4</sup>/  
lin.in.)

Inspection of equation 20 shows that ( $I$ ) varies with ( $H$ ) as a cubic function and, essentially, linearly with ( $T_o$ ); the term ( $T_o$ )<sup>3</sup> is small in comparison to ( $T_o$ ) because very thin plastic material is used. The inverse relationship between ( $P$ ) and ( $I$ ) is important to plastic-use efficiency. Thus, it appears that the values selected for ( $H$ ) and ( $P$ ) will be the most sensitive and will have the most effect on the resulting ( $I$ ) value. Specific examples illustrate this in step 7g.

**7b: Other computational formulae.**—To evaluate each trial corrugation profile, its parallel-plate, load-deflection resistance will be computed. The following equations are derived for this purpose.

For the case where  $NA \equiv E$  of the corrugation profile, which applies in this example (see fig. 4);

$$D_{NA} = D_i + H + T_o, \quad [21]$$

but by equations 13, with  $c = 2/3$  and  $D_i = 4.00$  in., equation 21 becomes

$$D_{NA} = 4.00 + H + 1.5 T_o; \text{ (in.)} \quad [22]$$

With the known values ( $E = 95,000$  p.s.i. from step 5 and  $\Delta y = 0.185$  in. from step 4) substituted into equation 1, ( $W$ ) can be computed from

$$W = \frac{12 EI \Delta y}{0.149 \left( \frac{D_{NA}}{2} \right)^3} = \frac{(12)(95,000)(0.185)(8)}{0.149} \cdot \frac{I}{D_{NA}^3} \quad [23]$$

or

$$W = (11,323,514) \frac{I}{D_{NA}^3}; \text{ (lb./lin. ft.)} \quad [24]$$

### 7c: Generation of design selection data.—

This phase of the design analysis requires some judgment in order to select suitable ranges for the variables ( $P$ ,  $H$ , and  $T_o$ ) which will provide a corrugation profile with the required ( $I_r$ ) value. For this example, the values in table 1 are considered.

When the trial values for  $P$ ,  $H$ , and  $T_o$  in table 1 were substituted into equations 20, 22, and 24, the corresponding values of  $I$ ,  $D_{NA}$ , and  $W$  were computed, tabulated in table 2, and presented graphically in figure 5. These data can be generated easily on many programmable office computers.

In figure 5, the graphical solution for the precise depth of corrugation ( $H$ ) for each pitch ( $P$ ) and material thickness ( $T_o$ ) is easily obtained, which will make a tube that can support the design load ( $W = 38.4$  lb./ft.) at the specified deflection ( $\Delta y = 0.185$  in.) between parallel plates. Thus, for the design example, 12 specific corrugation profiles are selected for further analysis and evaluation; the general parameters of these profiles are given in table 3.

**7d: Estimating tubing weight.**—To aid in evaluating the plastic-use efficiency for tubing made

TABLE 1.—Design example input for computing ( $I$ ) and ( $W$ ) of corrugated tubes with trial corrugations:  $D_i = 4$ -inch tubing

[3 × 3 × 4 = 36 combinations]

Variables	Trial values in inches		
$P$ .....	0.50	0.75	1.00
$H$ .....	.15	.20	.25
$T_o$ .....	.015	.020	.025
		.030	

\* The shaded equation numbers indicate equations used in computations for the design example.

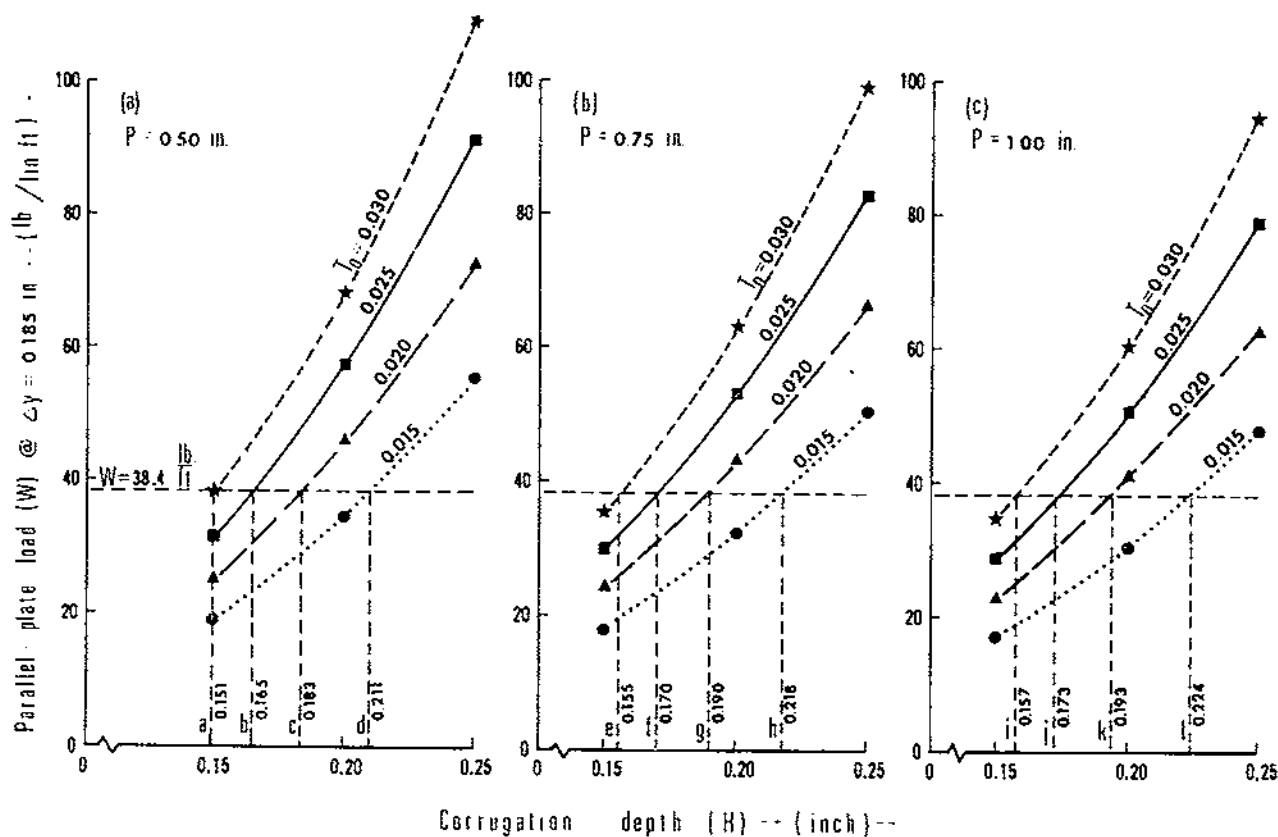


Figure 5. — Tubing parallel-plate load resistance ( $W$ ) for trial corrugation profiles.

with the various trial corrugation profiles, the unit weight of the tubing is approximated; computational equations for this purpose are derived below.

The cross-sectional area ( $A_w$ ) of the tubing's corrugated wall, per unit length of tube, can be calculated as follows (ref. to fig. 4(B) for definitions of terms):

$$A_w = \frac{1}{P} (L_o T_o + L_i T_i + 2T_w H); \left( \frac{\text{in.}^2}{\text{lin. in.}} \right) \quad [25]$$

But by the use of equations 12, 13, 14, 15, and 17, this expression can be simplified to

$$A_w = \left[ \left( \frac{2}{1+c} \right) + \left( \frac{1+c}{c} \right) \cdot \frac{H}{P} \right] (T_o) \quad [26]$$

For the design example, with  $c=2/3$ , equation 26 becomes

$$A_w = \left[ 1.2 + (2.5) \frac{H}{P} \right] (T_o); \left( \frac{\text{in.}^2}{\text{lin. in.}} \right) \quad [27]$$

It follows that the volume ( $v$ ) of plastic material per unit length of drain tubing can be computed as

$$v = \pi D_{NA} A_w; \left( \frac{\text{in.}^3}{\text{lin. in.}} \right) \quad [28]$$

and then the tubing unit weight ( $w$ ) can be calculated from the expression

$$w = 12v \rho_p \gamma_{H_2O} = 12\pi D_{NA} A_w \rho_p \gamma_{H_2O}; \left( \frac{\text{lb.}}{\text{lin. ft.}} \right)^{10} \quad [29]$$

where,

<sup>10</sup> Expressing the tubing weight per linear foot is a common practice.

$\rho_p \triangleq$  specific gravity of plastic material;

thus equation 29 becomes

$\gamma_{H_2O} \triangleq$  density of water; (lb./in.<sup>3</sup>)

$$W = 1.305 D_{NA} A_w \left( \frac{\text{lb.}}{\text{lin. ft.}} \right)$$

For the design example here,

$$\rho_p = 0.959$$

$$\gamma_{H_2O} = 0.0361 \text{ lb./in.}^3 @ 4^\circ \text{ C.}$$

**7e: Tube-wall stress analysis.**—The selection of the 12 corrugation profiles, presented in table 3, is based on the assumption that the maximum stress of the plastic material in the tube wall is within the linear range; that is, less than or equal

TABLE 2.—Design example trial corrugation evaluation data

Corrugation Code No.	P (in.)	H (in.)	T <sub>o</sub> (in.)	l (× 10 <sup>-4</sup> ) (in./lin. in.)	D <sub>NA</sub> (in.)	W <sup>1</sup> (lb./lin. ft.)
1.....	0.50	0.15	0.015	1.22	4.17	19.0
2.....	.50	.15	.020	1.64	4.18	25.5
3.....	.50	.15	.025	2.06	4.19	31.8
4.....	.50	.15	.030	2.49	4.20	38.2
5.....	.50	.20	.015	2.30	4.22	34.6
6.....	.50	.20	.020	3.07	4.23	46.0
7.....	.50	.20	.025	3.85	4.24	57.4
8.....	.50	.20	.030	4.64	4.25	68.8
9.....	.50	.25	.015	3.79	4.27	55.1
10.....	.50	.25	.020	5.06	4.28	73.2
11.....	.50	.25	.025	6.33	4.29	91.1
12.....	.50	.25	.030	7.62	4.30	109.1
13.....	.75	.15	.015	1.15	4.17	18.0
14.....	.75	.15	.020	1.55	4.18	24.1
15.....	.75	.15	.025	1.94	4.19	30.0
16.....	.75	.15	.030	2.34	4.20	35.9
17.....	.75	.20	.015	2.13	4.22	32.1
18.....	.75	.20	.020	2.85	4.23	42.7
19.....	.75	.20	.025	3.57	4.24	53.2
20.....	.75	.20	.030	4.30	4.25	63.7
21.....	.75	.25	.015	3.46	4.27	50.3
22.....	.75	.25	.020	4.63	4.28	67.0
23.....	.75	.25	.025	5.79	4.29	83.3
24.....	.75	.25	.030	6.97	4.30	99.7
25.....	1.00	.15	.015	1.12	4.17	17.5
26.....	1.00	.15	.020	1.50	4.18	23.3
27.....	1.00	.15	.025	1.88	4.19	29.0
28.....	1.00	.15	.030	2.27	4.20	34.9
29.....	1.00	.20	.015	2.05	4.22	30.9
30.....	1.00	.20	.020	2.74	4.23	41.0
31.....	1.00	.20	.025	3.44	4.24	51.3
32.....	1.00	.20	.030	4.14	4.25	61.4
33.....	1.00	.25	.015	3.30	4.27	48.0
34.....	1.00	.25	.020	4.41	4.28	63.8
35.....	1.00	.25	.025	5.52	4.29	79.4
36.....	1.00	.25	.030	6.64	4.30	95.0

<sup>1</sup> For  $\Delta y = 0.185$  in. and  $E = 95,000$  p.s.i. HDPE.

TABLE 3.—Design example corrugation profiles which will provide the required tube strength  $(W/\Delta y)^1$

Corrugation profile code <sup>2</sup>	<i>P</i>	<i>H</i>	<i>T<sub>v</sub></i>
	<i>inch</i>	<i>inch</i>	<i>inch</i>
a.....	0.50	0.151	0.030
b.....	.50	.165	.025
c.....	.50	.183	.020
d.....	.50	.211	.015
e.....	.75	.155	.030
f.....	.75	.170	.025
g.....	.75	.190	.020
h.....	.75	.218	.015
i.....	1.00	.157	.030
j.....	1.00	.173	.025
k.....	1.00	.193	.020
l.....	1.00	.224	.015

<sup>1</sup>  $W = 38.4 \pm 0.2$  lb./ft. @  $\Delta y = 0.185$  in. for each profile listed; this was checked by computer. (See fig. 5.)

<sup>2</sup> Note: All these tubes have the same conduit stiffness  $\left[ \frac{EI}{D_{NA}^3} \right]$  as defined below equation 2.

to the proportional limit. The validity of this assumption must be checked for each trial corrugation profile. Under the conditions of the design soil load and allowable tube deflection, the amount of stress in each tube's wall can be analytically determined as follows.

First, the *pure ring-compression* stress ( $\sigma_c$ ) in the tube wall, due to the overburden soil load ( $W_c$ ) is considered. A simplified, free-body diagram of the top half of the drain tube is shown in figure 6. The frictional forces between the outside of the tube wall and the surrounding soil are considered small and, thus, are neglected. It follows that the compressive tube walls at sides of the tube (see fig. 6) is

$$\sigma_c = \frac{W_c}{24A_w} \text{ (p.s.i.)} \quad [31]$$

For the design example being used here,  $W_c = 500$  lb. (see step 2), thus equation 31 becomes

$$\sigma_c = \frac{20.83}{A_w} \text{ (p.s.i.)} \quad [32]$$

where ( $A_w$ ) is in units of  $\left( \frac{\text{in.}^2}{\text{lin. in.}} \right)$ , on one side of the tubing only, for each trial corrugation to be considered.

Next, the *bending stress* ( $\sigma_B$ ) resulting from the deflection ( $\Delta x_s$ ) of the corrugated tube wall is considered. It is desirable to express ( $\sigma_B$ ) directly as a function of ( $\Delta x_s$ ); that is,

$$\sigma_B = f(\Delta x_s) \quad [33]$$

To derive an expression for the function indicated by equation 33, the following simplifying assumption is made: Soil loading will cause the same bending stress ( $\sigma_B$ ) in the side-wall of the corrugated tube as parallel-plate loading, provided the same tube deflection is produced by each of the two types of loading; that is, *only* if  $\Delta x_s \equiv \Delta x$ . For simple analysis, parallel-plate loading is considered for finding ( $\sigma_B$ ), as shown in figure 7.

Basic engineering mechanics of bending stress in beams (3), show that

$$\sigma_B = \frac{MC}{I} \quad [34]$$

where,

$\sigma_B \triangleq$  bending stress, (p.s.i.);

$M \triangleq$  bending moment, (in.-lb.),<sup>11</sup> at cross section being considered (see fig. 7, b);

$C \triangleq$  distance from  $NA$  to outermost beam fiber, (inch);

$I \triangleq$  moment-of-inertia of cross section, (in.<sup>4</sup>).<sup>11</sup>

Specifically, for the conditions shown in figure 7(b), an expression for the bending moment ( $M$ ) in the tube wall, for small deflections, is given by Boyd (3, p. 358) as

$$M = 0.1817 \left( \frac{D_{NA}}{2} \right) \left( \frac{W}{12} \right); \left( \frac{\text{in.-lb.}}{\text{lin. in.}} \right) \quad [35]$$

Now, solve equation 2 for ( $W$ ) and substitute into equation 35;

<sup>11</sup> This is for a definite beam width; for an indefinitely wide beam, as in the corrugated wall of the continuous tube, the units would be

$\left( \frac{\text{in.-lb.}}{\text{in. of width}} \right)$  for  $M$ , and  $\left( \frac{\text{in.}^4}{\text{in. of width}} \right)$  for  $I$ .

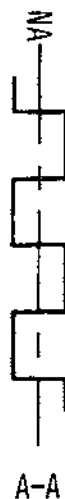
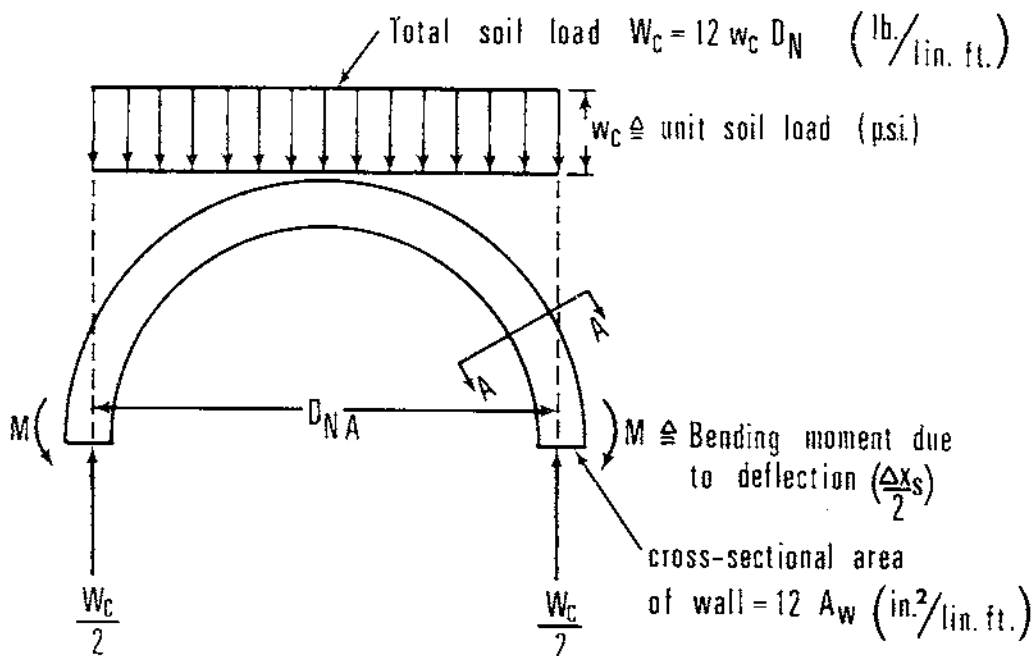


Figure 6. — Free-body diagram for top half of draitube under design soil load ( $W_c$ ).

$$M = 5.33 \left( \frac{EI \Delta x}{D_{NA}^2} \right); \left( \frac{\text{in.} \cdot \text{lb.}}{\text{lin. in.}} \right) \quad [36]$$

For the design example here, with  $E = 95,000$  p.s.i.,  $\Delta x = 0.17$  in., and  $c = 2/3$ , equation 38 becomes

$$\sigma_B = 42,959 \left[ \frac{H + 1.5T_o}{D_{NA}} \right]; \text{ (p.s.i.)} \quad [40]$$

Equation 36 is substituted into 34, the units of ( $I$ ) as ( $\text{in.}^4/\text{lin. in.}$ ) are considered as required in analyzing the corrugated wall of a continuous tube, and the value of ( $C$ ) is set as

$$C \triangleq \frac{H}{2} + \frac{T_i}{2} = \frac{1}{2} \left( H + \frac{T_o}{c} \right), \quad [37]$$

The maximum *total stress* ( $\sigma_{TC}$ ) in the tube wall can now be determined as shown vectorially in figure 8.

to obtain the desired expression for ( $\sigma_B$ ); that is

Because the pure compressive stress ( $\sigma_c$ ) adds to the compressive component of the bending stress ( $\sigma_{BC}$ ), the critical or maximum stresses in the corrugated tube walls are *compressive*. The stresses occur on the inside tube diameter (roots of the corrugations) at the sides of the tube and on the outside tube diameter (ridges of corrugations) at the top and bottom of the tube (see fig. 9).

$$\sigma_B = 2.66 \left[ \frac{E \left( H + \frac{T_o}{c} \right)}{D_{NA}^2} \right] (\Delta x); \text{ (p.s.i.)} \quad [38]$$

Therefore, the tube-wall stress analysis and design relationship of importance is

Note that

$$2.66 \left[ \frac{E \left( H + \frac{T_o}{c} \right)}{D_{NA}^2} \right] = \text{constant} \quad [39]$$

$$\sigma_{max} = \sigma_{TC} = \sigma_c + \sigma_{BC}. \quad [41]$$

for any given corrugation profile being considered; thus, the condition of equation 33 is satisfied.

For an acceptable corrugation design, maximum stress should be less than or equal to the propor-

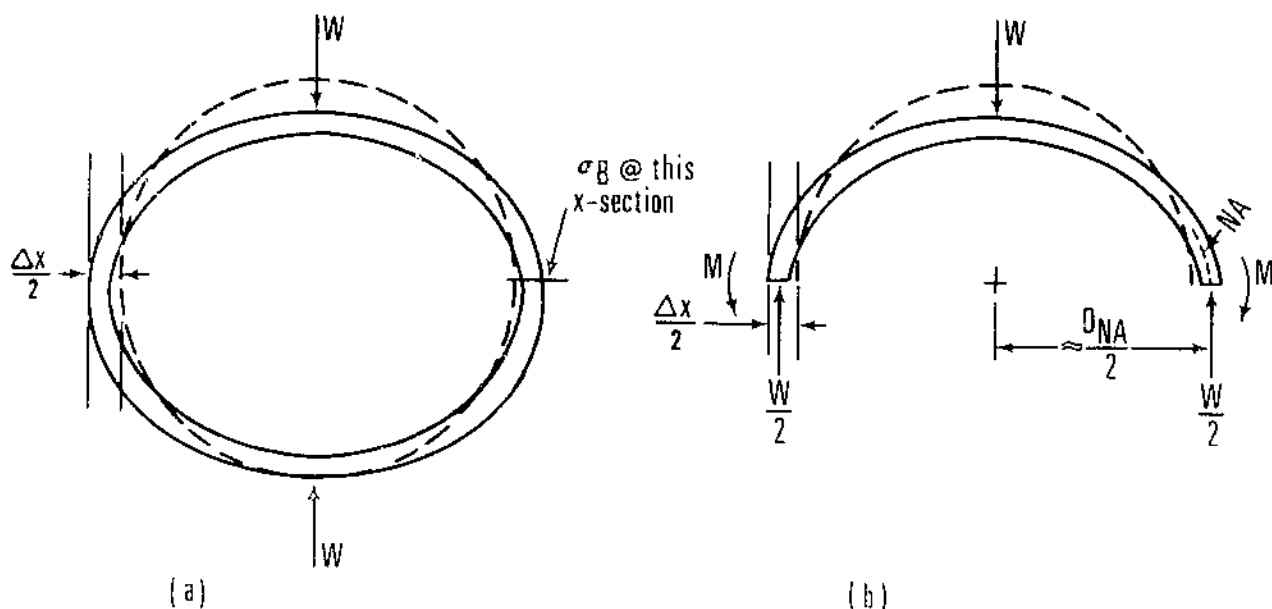


Figure 7.—Bending stress ( $\sigma_B$ ) analysis based on parallel-plate load-deflection ( $\frac{W}{\Delta X}$ ).

tional limit stress ( $\sigma_{pl}$ ) for the particular plastic material being used; mathematically, that is

$$\sigma_{TC} \cong \sigma_{pl}. \quad [42]$$

Stresses in either tension ( $T$ ) or compression ( $C$ ) above ( $\sigma_{pl}$ ) is considered to cause *nonlinear deflection* of the draitube.

For several plastic materials, including *HDPE* and *PVC*, a rule-of-thumb assumption (1, 14) for design purposes is to set the proportional limit stress ( $\sigma_{pl}$ ) at about one-third the yield-point stress ( $\sigma_{YP}$ );

$$\sigma_{pl} \approx \frac{1}{3} \sigma_{YP}. \quad [43]$$

For the design example here, however, ( $\sigma_{pl}$ ) is estimated from the stress-strain data presented in Appendix I, or

$$\sigma_{pl} \approx 1,000 \text{ p.s.i.} \quad [44]$$

for a proportional limit strain ( $\epsilon_{pl}$ ) of nearly 1 percent. Therefore, equation 42 becomes

$$\sigma_{TC} \cong 1,000 \text{ p.s.i.} \quad [45]$$

Next, for draitubes with corrugations determined by equation 42, the exact deflection ( $\Delta x_{pl}$ ) at which the tubewall stress ( $\sigma_{TC}$ ) equals ( $\sigma_{pl}$ ) is needed. For example, this information will provide the factor-of-safety that is available when the draitube is deflected more than the design level ( $\Delta x_s$ ) by such conditions as concentrated loads from soil clods or stones in the ditch backfill material. The recommended method for computing ( $\Delta x_{pl}$ ) is:

$$\sigma_{TC} = \sigma_{pl} = \sigma_{B_{pl}} + \sigma_c, \quad [46]$$

where ( $\sigma_c$ ) is the same as determined previously by the use of equation 31; the unknown bending stress ( $\sigma_{B_{pl}}$ ) can be determined from equation 46 as

$$\sigma_{B_{pl}} = \sigma_{pl} - \sigma_c. \quad [47]$$

In the design example, with  $\sigma_{pl} = 1,000$  p.s.i., equation 47 becomes

$$\sigma_{B_{pl}} = 1,000 - \sigma_c; \text{ (p.s.i.)} \quad [48]$$

Only linear tube deflections are considered, so the value of ( $\Delta x_{pl}$ ) can be obtained by a ratio relation-

ship from the previous results for design load and deflection conditions; that is,

$$\frac{\Delta x}{\sigma_B} = \frac{\Delta x_{pl}}{\sigma_{Bpl}} \quad [49]$$

where, ( $\Delta x$ ) is the value determined from equation 2 and ( $\sigma_B$ ) as determined in equation 38, both for the design parallel-plate load ( $W'$ ). When equation 49 is solved for ( $\Delta x_{pl}$ ),

$$\Delta x_{pl} = \left( \frac{\Delta x}{\sigma_B} \right) \sigma_{Bpl}; \text{ (inch).} \quad [50]$$

For the design example herein, with  $\Delta x = 0.17$  in. and with equation 48 substituted for ( $\sigma_{Bpl}$ ), equation 50 becomes

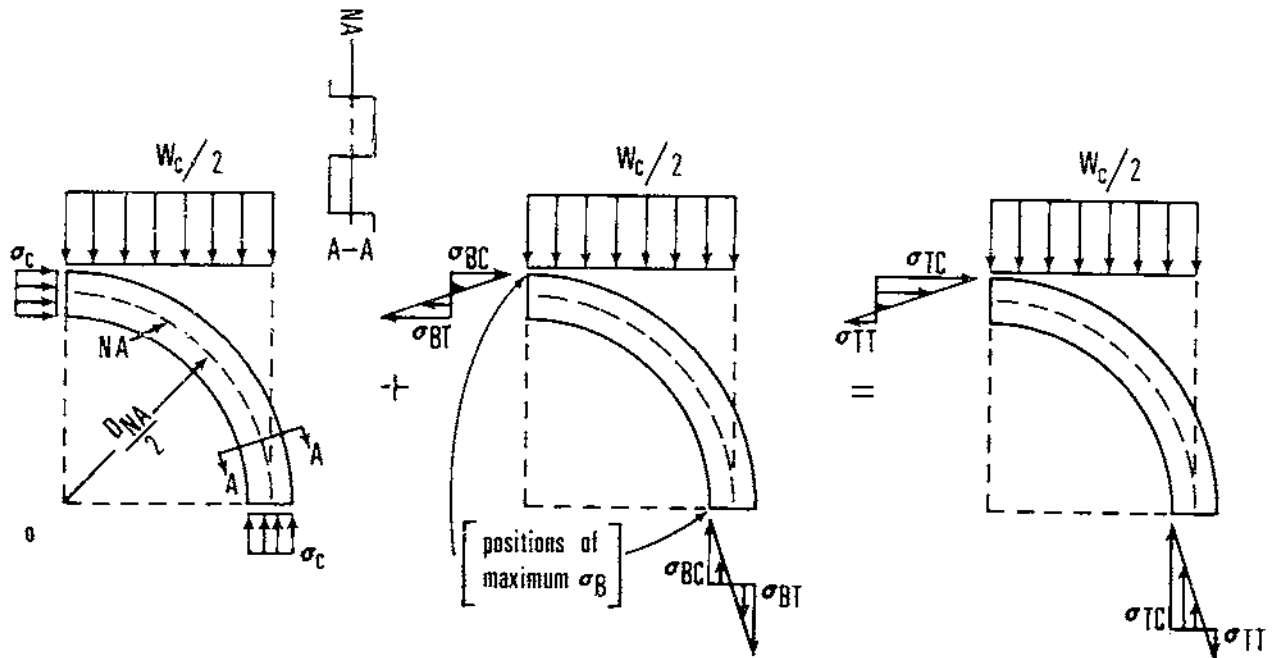
$$\Delta x_{pl} = \left( \frac{0.17}{\sigma_B} \right) (1,000 - \sigma_c); \text{ (inch).} \quad [51]$$

Because the corrugated tubing should deflect more than the design limit (that is,  $\Delta x_{pl} > \Delta x$ ) without excessive stress buildup in the tube walls (that is,  $\sigma_{rc} \leq \sigma_{pl}$ ), and because the tubing should be lightweight, a corrugation profile can be selected by the computation of the following factors.

Plastic-use-efficiency factor

$$\underline{\Delta} \left[ \frac{\Delta x_{pl}}{w} \right]; \left( \frac{\text{in.}}{\text{lb./in. ft.}} \right) \quad [52]$$

where ( $w$ ) is the unit weight determined with equation 29 for each trial corrugation.

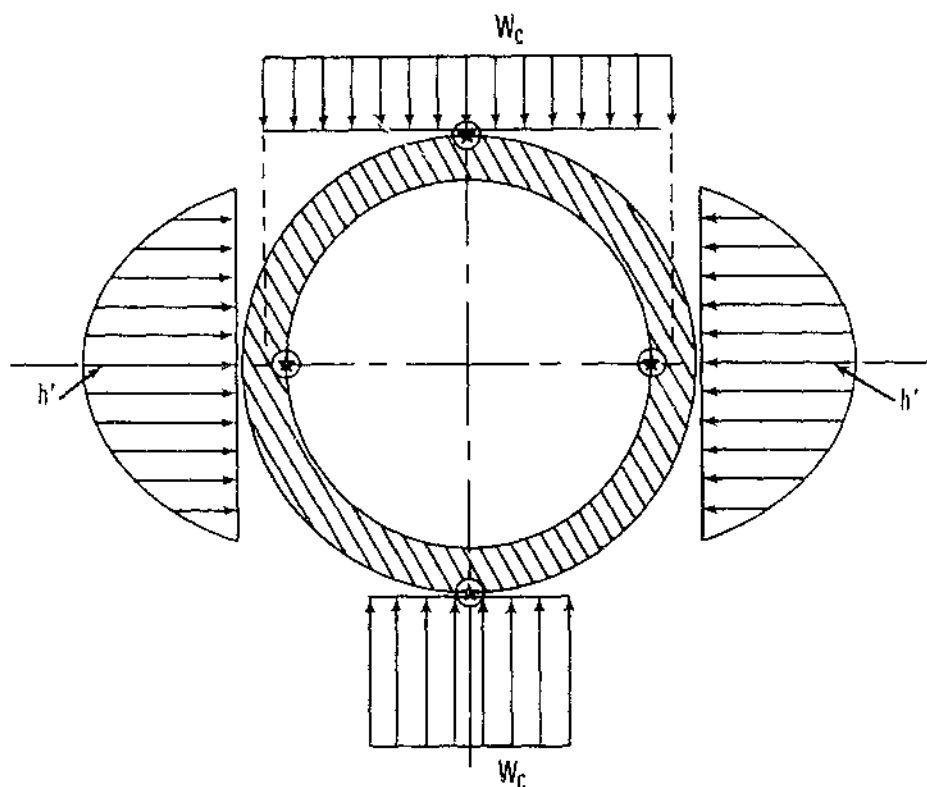


That is:

Component of wall stress in pure compression	+	Component of wall stress in bending: BC = compression; BT = tension	=	Vector sum of wall stresses
$\bar{\sigma}_c$	+	$\bar{\sigma}_B$	=	$\bar{\sigma}_T$

Figure 8. —Major stress components in the tube wall, caused by overburden soil load and by tube deflection.





Points of maximum tube wall compressive stress marked with ★.

Note: The same critical stress points occur for parallel-plate loading.

Figure 9.—Critical or maximum stress points in corrugated tube wall for soil loading conditions.

The final part of tube-wall stress analysis involves the approximation of *shear stress* level ( $\sigma_s$ ) in the corrugation webs, illustrated in figure 10.

The total *shear force* ( $S$ ) per corrugation web and one quadrant of tube circumference can be approximated in the following simplified manner:<sup>12</sup>

$$S = \left( \frac{2}{3} \sigma_{B_{pl}} \right) \left( \frac{A_w P}{4} \right); \text{ (lb.)}, \quad [53]$$

where  $\sigma_{B_{pl}}$  is the maximum bending stress per equation 47 for design conditions (p.s.i.), and  $\left( \frac{A_w P}{4} \right)$  = one-fourth the cross-sectional area of one corrugation pitch (in.<sup>2</sup>). The shear area ( $A_s$ ) for one web over a quadrant of the tube circumference is

$$A_s = \left( \frac{\pi D_{N1}}{4} \right) T_w, \quad [54]$$

or with the use of equation 17

$$A_s = \left[ \frac{\pi(1+c)}{8c} \right] D_{N1} T_w; \text{ (in.<sup>2</sup>)}. \quad [55]$$

Thus, the shear stress ( $\sigma_s$ ) can be computed from equations 53 and 55 as

$$\sigma_s = \frac{S}{A_s}; \text{ (p.s.i.)} \quad [56]$$

For the design example, where  $c=2/3$ , equation 56 can be written, following substitution of equations 53 and 55,

$$\sigma_s = (0.17) \left[ \frac{(A_w P) \sigma_{B_{pl}}}{D_{N1} T_w} \right]; \text{ (p.s.i.)}. \quad [57]$$

#### 7f: Generation of design evaluation data.—

The computational equations developed in steps 7d and 7e can now be used to evaluate in depth the 12 corrugation profiles listed in table 3, before final selection of the profile for the design example

<sup>12</sup> A more rigorous analysis does not seem justified because the shear stresses are usually not high.

is made. The specific equations for continuing the design example are 27, 30, 32, 40, 41, 48, 51, 52, and 57. A computer program, devised for solving these sets of equations, can be easily set up on many programmable office computers, such as the Olivetti-Underwood, Programma 101 computer.<sup>13</sup> Results of all computations relative to the design example are given in table 4.

**7g: Selection of corrugation profile.**—Several methods can be used to summarize or interpret the design evaluation data in table 4 to arrive at the final selection of corrugation profile. However, the presentation of certain factors and parameters in figures 11 and 12 for the design example has been especially helpful. Specifically, an isometric graph, plotted to relate  $P$ ,  $H$ , and  $w$  for different values of  $T_0$ , provides a design surface

<sup>13</sup> Trade names are used in this publication solely for the purpose of providing specific information. Mention of a trade name does not constitute a guarantee or warranty of the product by the U.S. Department of Agriculture or an endorsement by the Department over other products not mentioned.

(as shown in fig. 11) from which the lightest weight ( $w$ ) tubing is obtained for  $P=1.00$  in. and  $T_0=0.015$  in. (Note:  $P=1.00$  in. is considered the maximum practical value for pitch, and  $T_0=0.015$  in. is considered about the minimum reliable value for wall thickness. These values are based on previous extruding experience with HDPE plastic tubing.) The meaning of design surface is that any point on the surface (as defined by its coordinates  $P$ ,  $H$ , and  $w$ , which also imply a specific value for  $T_0$ ) will provide a 4-inch corrugated-wall tube with the required parallel-plate, load-deflection strength— $W=38.4\pm 0.2$  lb./ft. @  $\Delta y=0.185$  in. At this step in the design procedure, a corrugation profile can be selected from the design surface which will require a specified weight of plastic material for fabricating the draintube (see the lines of constant tube weight ( $w$ ) drawn on the design surface in figure 11). However, in the discussion of the design example, only the 12 special corrugations listed in table 3 are considered here. This procedure illustrates some of the types of analyses and practical considerations that are involved in selecting tube designs of different weights.

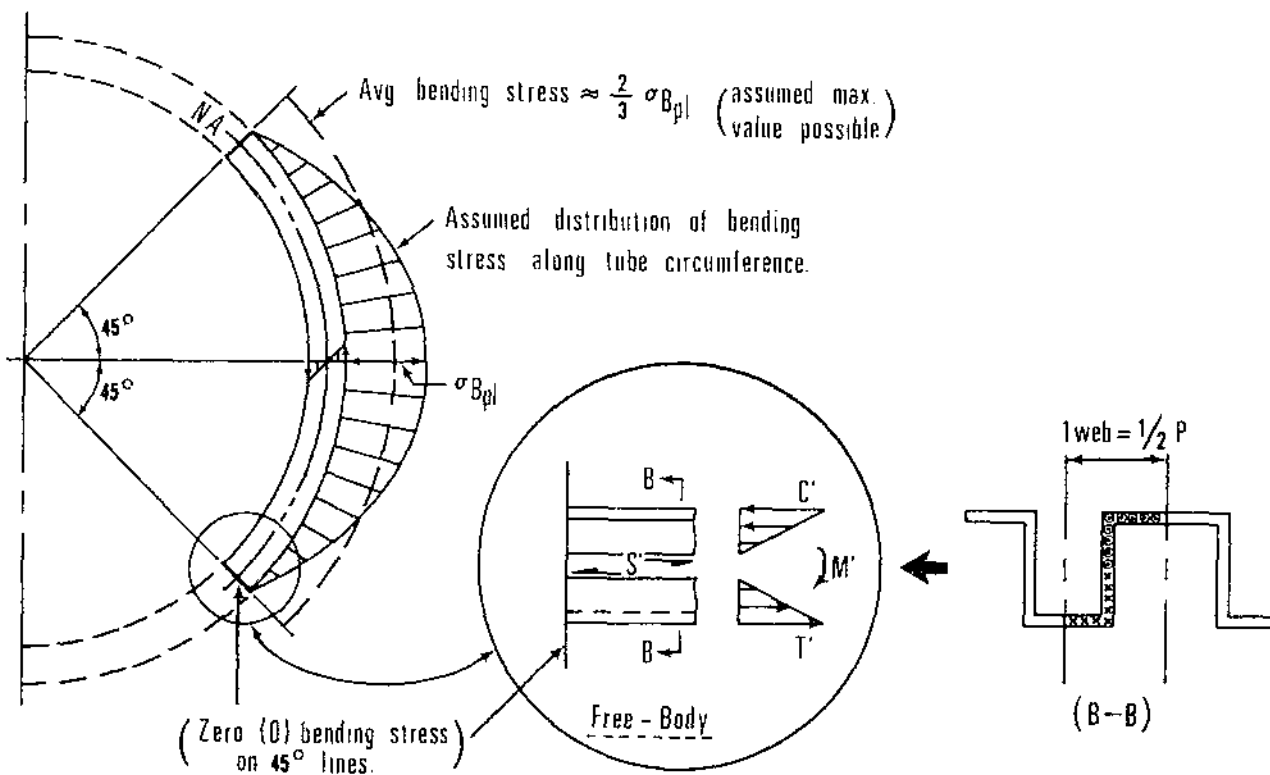


Figure 10.—Assumed distribution of bending stress in tube walls causing shear forces in the corrugation webs.

TABLE 4.—Example design evaluation data of proposed wall corrugation profiles<sup>1</sup> for 4-inch diameter draitubing

Corrugation code	$P$ (in.)	$H$ (in.)	$T_o$ (in.)	$T_I$ (in.)	$L_o$ (in.)	$L_I$ (in.)	$D_{NA}$ (in.)	$A_w$ (in. <sup>2</sup> ) ( $\times 10^{-2}$ )	$w$ (lb./ft.) <sup>2</sup>	$\sigma_c$ (p.s.i.) <sup>2</sup>	$\sigma_R$ (p.s.i.) <sup>2</sup>	$\sigma_{TC}$ (p.s.i.) <sup>2</sup>	$\sigma_{Bpl}$ (p.s.i.) <sup>4</sup>	$\Delta x_{pl}$ (in.)	$\Delta x_{pl}/w$ (in./lb./ft.)	$\sigma_s$ (p.s.i.)
a.....	0.50	0.151	0.030	0.045	0.30	0.20	4.20	5.86	0.32	355	478	833	645	0.23	0.71	26
b.....	.50	.165	.025	.037	.30	.20	4.20	5.06	.28	411	493	904	589	.20	.73	24
c.....	.50	.183	.020	.030	.30	.20	4.21	4.23	.23	492	516	1,008	508	.17	.72	22
d.....	.50	.211	.015	.023	.30	.20	4.23	3.38	.19	616	560	1,176	384	.12	.62	17
e.....	.75	.155	.030	.045	.45	.30	4.20	5.15	.28	404	487	891	596	.21	.74	31
f.....	.75	.170	.025	.037	.45	.30	4.21	4.42	.24	472	503	975	528	.18	.74	28
g.....	.75	.190	.020	.030	.45	.30	4.22	3.67	.20	568	531	1,099	432	.14	.69	24
h.....	.75	.218	.015	.023	.45	.30	4.24	2.89	.16	721	574	1,295	279	.08	.52	16
i.....	1.00	.157	.030	.045	.60	.40	4.20	4.78	.26	436	491	927	564	.20	.74	36
j.....	1.00	.173	.025	.037	.60	.40	4.21	4.08	.22	510	510	1,020	490	.16	.73	32
k.....	1.00	.193	.020	.030	.60	.40	4.22	3.36	.19	619	537	1,156	381	.12	.65	26
l.....	1.00	.224	.015	.023	.60	.40	4.25	2.64	.15	789	587	1,376	211	.06	.42	15

<sup>1</sup> All tubes listed are for HDPE, Type III plastic, with  $E = 95,000$  p.s.i. and meet parallel-plate strength-deflection requirement; that is,  $W = 38.4 \pm 0.2$  lb./ft. @  $\Delta y = 0.185$  in.

<sup>2</sup> Specific gravity = 0.959; HDPE.

<sup>3</sup> For  $W_c = 500$  lb./ft. @  $\Delta x_1 = 0.17$  in.

<sup>4</sup> For deflection =  $\Delta x_{pl}$ .

The results of the tube-wall stress analysis (step 7e and table 4,  $\sigma_{TC}$ ) are used to truncate the design surface for deleting those corrugation profiles for which the wall stress exceeds the proportional limit at the design tube deflection (that is,  $\sigma_{TC} > \sigma_{pl} \approx 1,000$  p.s.i. @  $\Delta x = 0.17$  in.); see truncation-plane in figure 11. Thus, for the design example, the design surface was restricted so that only the following six corrugation profiles were structurally acceptable for use: Corrugation profile codes *a*, *b*, *c*, *e*, *f*, and *i* (see final design surface in fig. 11). Note that, in the section from these profiles, *c*, *f*, and *i* are lowest in weight (*w*). In terms of plastic-use-efficiency

(defined as the  $\left[\frac{\Delta x_{pl}}{w}\right]$  ratio), the same three profiles are the most efficient, as shown in figure 12. Therefore, the final selection is made between profiles *c*, *f*, and *i*. Specific comparisons are as follows:

*Wall-profile (c)* provides the lightest draitube at  $w_{(c)} = 0.23$  lb./ft. To obtain a better perspective of the significance of tubing weight in this comparative analysis, a *cost* estimate (\$) for the tubing is made on the basis of 40¢/lb.;<sup>14</sup> thus,  $\$_{(c)} = 0.40 \times 0.23 =$

<sup>14</sup>This was a typical selling price for 4-inch, corrugated plastic drainage tubing on the U.S.A. market in 1969-70.

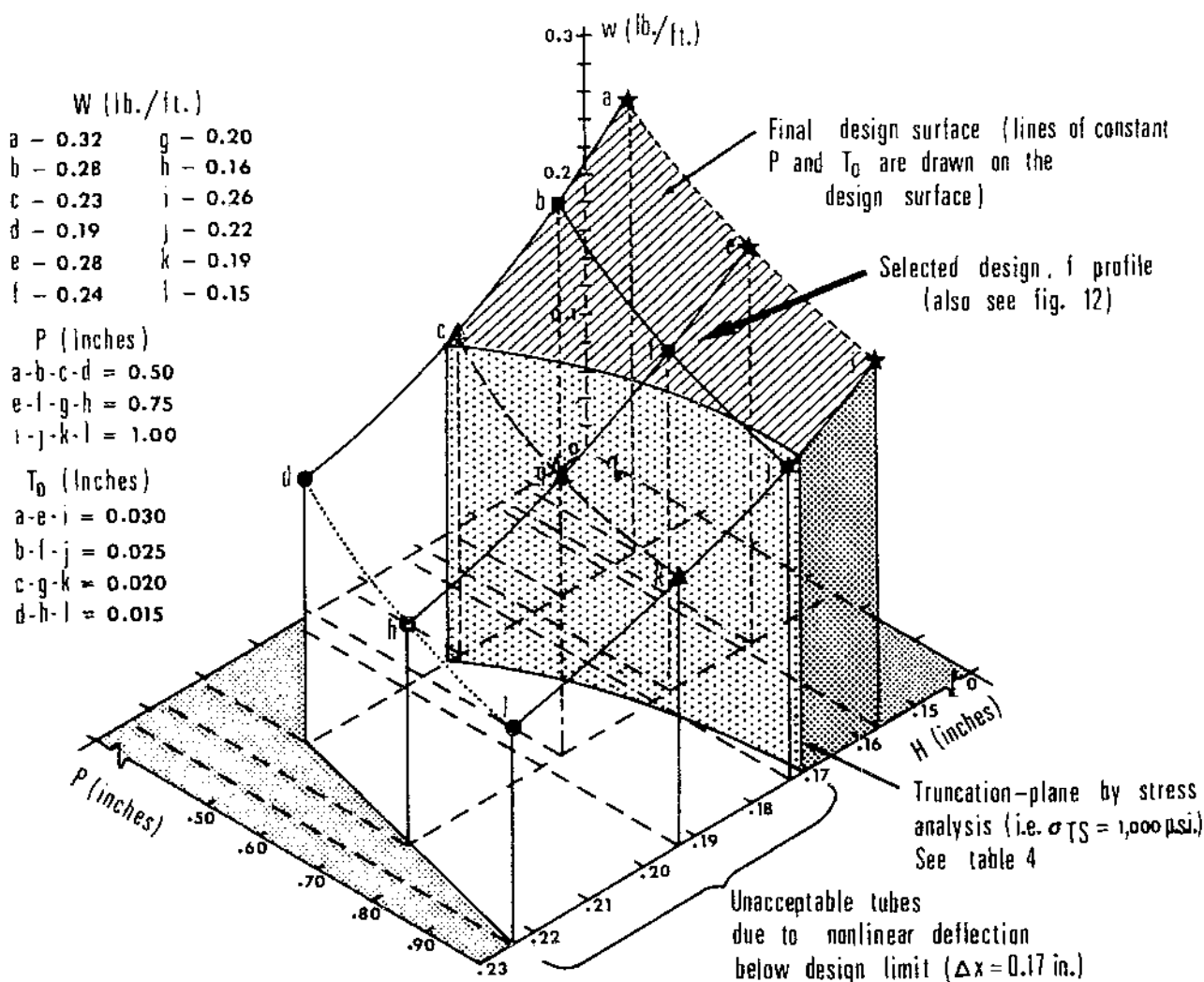


Figure 11.—Design Surface relating *P*, *H*,  $T_0$ , and *w* of trial corrugations which meet the 4-inch tube strength-deflection requirement (that is,  $W = 38.4 \pm 0.2$  lb./ft. @  $\Delta y = 0.185$  in. or  $\Delta x = 0.17$  in.). (Data from table 4.)

\$0.092 per lin. ft. But, note in table 4 that, for profile (c) tubing,  $\Delta x_{pl} \equiv \Delta x_{design} = 0.17$  inch.

Wall-profile (f) tubing would have a unit weight of  $w_{(f)} = 0.24$  lb./ft., which is about 4.3 percent heavier than profile (c) tubing;  $\$_{(f)} = 0.40 \times 0.24 = \$0.096$  per ft. However,  $\Delta x_{pl} = 0.18$  inch, which is greater ( $\Delta x_{design}$ ) by about 5.9 percent.

Wall-profile (i), similarly,  $w_{(i)} = 0.26$  lb./ft.  $\$_{(i)} = \$0.104$  per ft., or about 13 percent heavier and more costly than profile (c) tubing. And,  $\Delta x_{pl} = 0.20$  inch, which is greater than ( $\Delta x_{design}$ ) by about 17.6 percent.

Based on the above comparative analyses, plus some practical considerations that are spelled out in

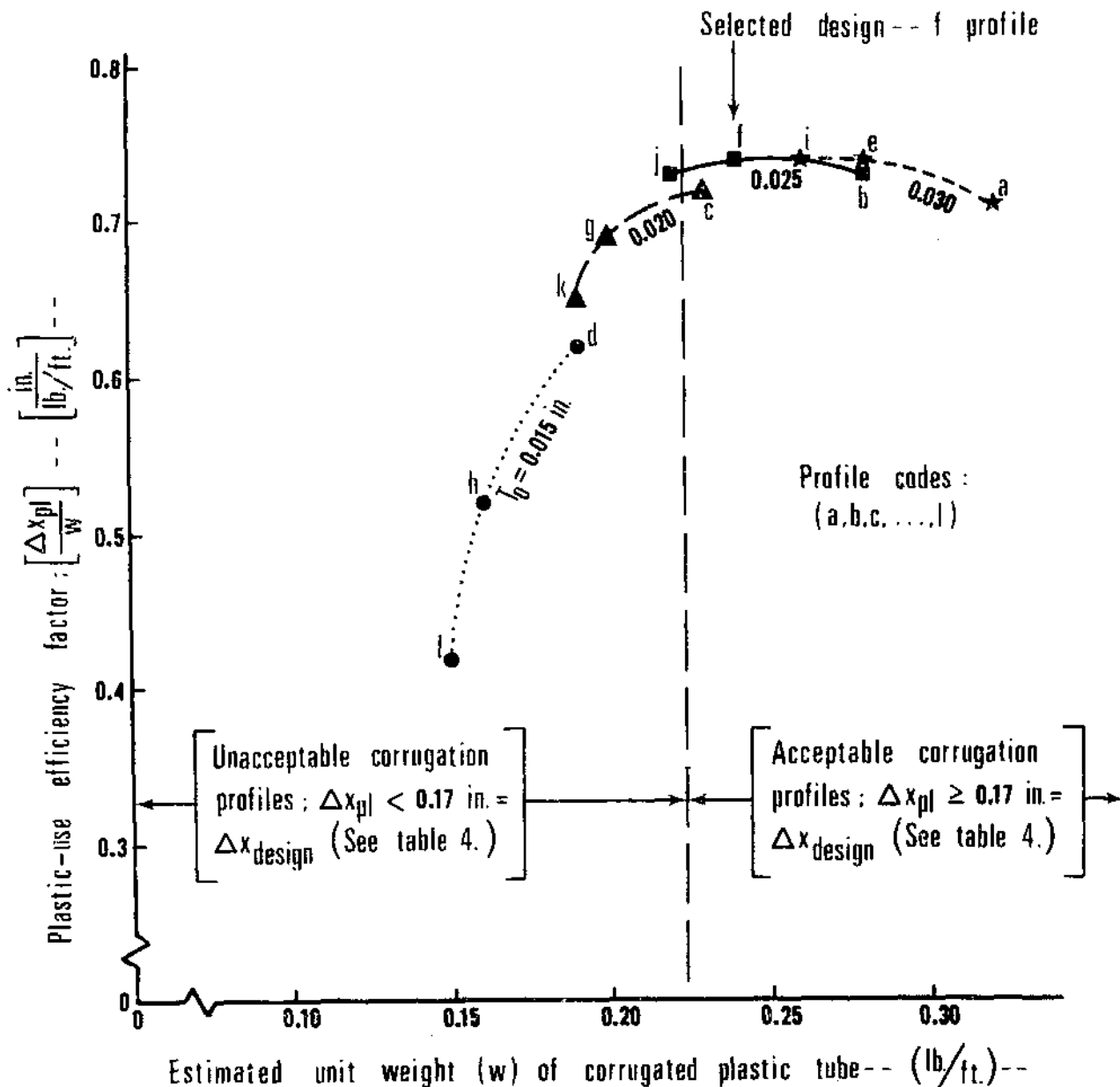


Figure 12. — Plastics use efficiency expressed as  $(\Delta x_{pl}/w)$  versus estimated corrugated tubing unit weight (w), for trial corrugation profiles. (Data from table 4.)

more detail below, the corrugation profile (*f*) is selected for use relative to the 4-inch draitube design example presented herein. Other factors considered in arriving at this decision are as follows:

(1) To provide some margin of safety in design, it is this author's judgment that  $(\Delta x_{pl})$  should be at least 5 to 10 percent greater than  $(\Delta x_{design})$  to insure that the parallel-plate, load-deflection requirement will be met by the fabricated tubing. (Profile *f*) satisfies this criterion.)<sup>15</sup>

(2) It is not considered necessary to require linear tube deflection in excess of that indicated in (1) because for HDPE, PVC, and many plastic materials, all strain up to nearly the yield point is recoverable if the load is removed (14). The discussion presented in step 2 shows the conduit loading is cyclic with the soil wetting and drying periods.

(3) The corrugation pitch of  $P = 0.75$  in. may make it easier to form the water-entry openings in the tube walls than if  $P = 0.50$  in. More detail is given in step 9.

(4) Accuracy and quality of tube-wall thickness may be easier to control when  $T_o = 0.025$  in. than when  $T_o = 0.020$  in.

(5) The additional projected cost of four-tenths

<sup>15</sup> Note: In figure 11 it can be seen that any corrugation profile on the design surface which will provide a tubing unit weight ( $w$ ) of about 0.24 lb./ft. will also satisfy this requirement—the lines of constant tubing weight ( $w$ ) are nearly parallel to the truncation-plane where  $\Delta x_{pl} = \Delta x_{design}$ .

of a cent per foot for profile (*c*) seemed to be justified in view of advantages (3) and (4) above.

The conclusion of step 7 is given in figure 13.

### Step 8: Approximating Minimum Coiling Radius for Draitube

Once the corrugation profile has been selected, approximating the smallest practical radius into which the draitube can be coiled is a simple task. Figure 14 shows the geometric basis for the approximation. In principle, the approximation involves calculating the coiling radius commensurate with some allowable stretching or shortening of one corrugation pitch. The analysis in this report is made on the basis of an allowable shortening of one corrugation pitch on the inside radius of the coil as shown in figure 14, detail (a).

An equation for computing ( $R_i$ ) is derived by letting

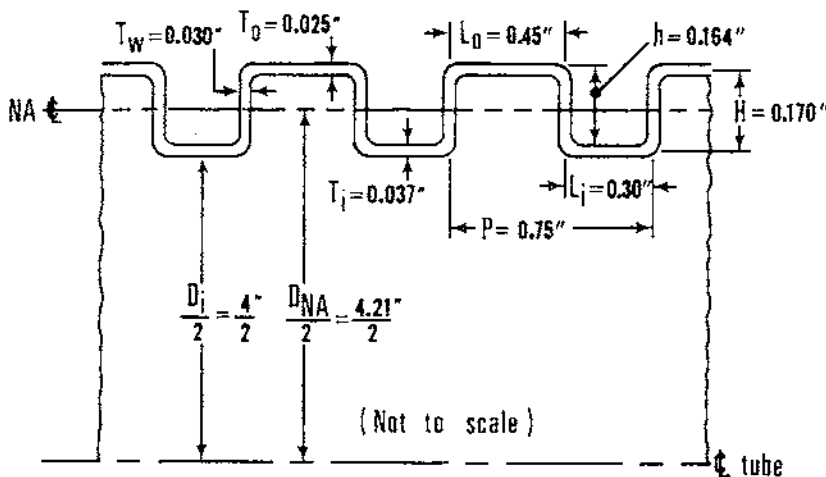
$$R_c \theta = P \quad [58]$$

at the  $q_c$  (axis) of the Corrugated tubing. At the inside coil radius ( $R_i$ ),

$$R_i \theta = P_i \quad [59]$$

Equations 58 and 59 are solved for ( $\theta$ ), and then the right-hand sides are equated:

$$\theta = \frac{P}{R_c} = \frac{P_i}{R_i} \quad [60]$$



#### Predicted performance specifications:

$W = 38.4$  lb./ft. parallel-plate  
@  $\Delta y = 0.185$  in. for  
 $E = 95,000$  p.s.i.

$w = 0.24$  lb./ft. for HDPE with  
specific gravity = 0.959

$\Delta x_{pl} = 0.18$  in. ( $\sigma_{pl} = 1,000$  p.s.i.)

Figure 13.—Selected corrugation profile (*f*) for design example 4-inch HDPE plastic draitube and predicted performance specifications.

but,

$$R_{\zeta} = R_i + \frac{D_{NA}}{2} \quad [61]$$

Now, equation 61 is substituted into 60; ( $P_i$ ) is expressed as shown in figure 14;  $P = L_i + L_o$  from equation 11; and when solved for ( $R_i$ ), gives

$$R_i = \left( \frac{P}{4H \sin \Phi} - \frac{1}{2} \right) D_{NA} \quad [62]$$

where ( $\Phi$ ) is defined in figure 14, detail (a).

In the case of the corrugation profile ( $f$ )—figure 13—selected as a part of the *design example*, where

$$P = 0.75 \text{ in.}; H = 0.170 \text{ in.}; D_{NA} = 4.21 \text{ in.},$$

and assuming  $\Phi = 15^\circ$ , from equation 62

$$R_{i(f)} = 15.9 \text{ inch} \approx C_{Rmin}.$$

That is, the plastic draitube with corrugation profile ( $f$ ) could be coiled onto a 30-inch-diameter mandrel or spool.

### Step 9: Water-Entry Openings in Draitube Wall

As a rule-of-thumb, the cross-sectional area of the water-entry openings in the tube wall of a 4-inch-diameter drain can be approximated at about 1.0 percent of the drain's outside wall circumferential area (18).<sup>16</sup> In the case of a corrugated-wall draitube, the neutral-axis diameter ( $D_{NA}$ ) may be used to compute the effective circumferential area of the tube wall.

The walls of the corrugated plastic draitube can be perforated for water entry by drilling or punching

<sup>16</sup>The amount of water entry opening area required varies considerably with drain diameter and depth of installation.

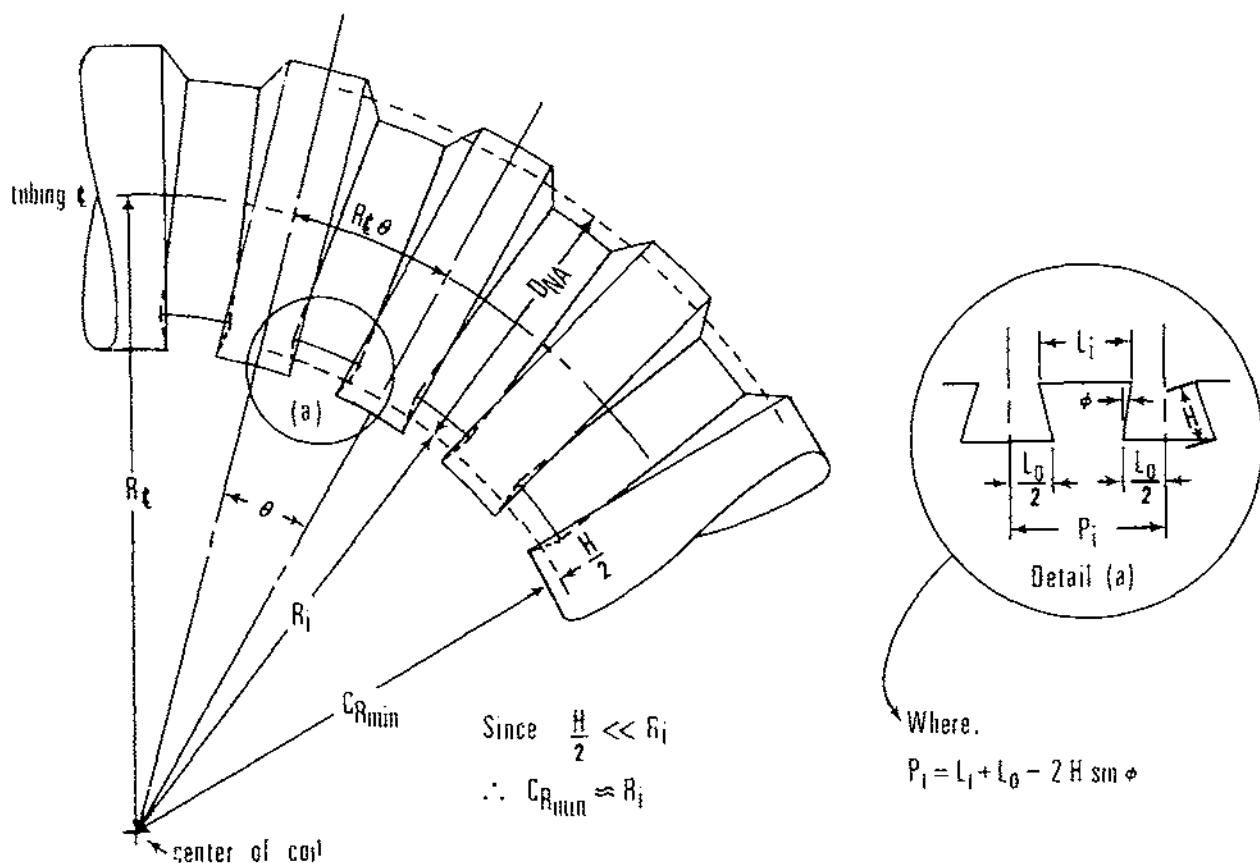


Figure 14. — Minimum coiling radius for corrugated plastic draitube.

holes or by sawing short narrow slots. To conserve structural strength of the corrugated wall, the openings can be made along the neutral axis of the corrugations and the draitube. However, because the openings are more difficult to make in the  $NA$  in the corrugation webs, the second best position is in the roots between the corrugation ridges. Slots sawed in the tube wall in the roots is the preferred way of forming the water entry openings as shown in figure 15. The slots should be made along the tube walls in an odd number of rows, such as, 3 and 5<sup>17</sup> evenly spaced around the tube circumference. They can be spaced longitudinally along the tube so that they occur only in every other or every third corrugation root (see fig. 15). This method will generally provide adequate tube-wall openings without unduly weakening the corrugated walls. The water-entry slots should be no wider than one-half the root width ( $L_r$ ), to minimize structural weakening of the corrugation. It is further recommended that the ends of each slot be rounded, or filleted with a round-tooth saw blade, in order to relieve stresses that occur when the tubing is coiled, especially at low temperatures.

This final step is conducted for the design ex-

<sup>17</sup>The odd number of rows is recommended in order to avoid simultaneous coincidence with the four critical stress points illustrated in figure 9.

ample presented; complete procedures and computations are given below (refer to fig. 13 for tube dimensions).

(a) Tube-wall circumferential area  $= A_{tw} = 12\pi D_{NA} = (12)(3.142)(4.21) = 159 \text{ in.}^2/\text{lin. ft.}$

(b) For the 4-inch ID draitube, assume 1 percent of  $A_{tw} = (0.01)(159) = 1.6 \text{ in.}^2/\text{lin. ft.}$  = total area of openings per foot of drain.

(c) For  $P = 0.75 \text{ in.}$ ; 16 corrugations/lin. ft. of tubing or corrugation roots/lin. ft.

(d) Consider tube-wall openings made by a *sawed slot* in every other corrugation root and in three rows along the tube ( $120^\circ$  intervals around the tube circumference).

(e) Therefore, the number of slots per foot of tubing  $= \frac{16}{2} \times 3 = 24 \text{ slots/lin. ft.}$

(f) Area for each slot  $= \frac{1.6 \text{ in.}^2}{24 \text{ slots}} = 0.067 \text{ in.}^2/\text{slot.}$

(g) Consider a slot width  $= 0.0625 \text{ in.}$  (which is  $< L_r = 0.300 \text{ in.}$ ).

(h) Then, length of each slot  $= \frac{0.067 \text{ in.}^2/\text{slot}}{0.065 \text{ in.}}$   
 $\approx 1.1 \text{ in. length/slot}$ , which is a practical dimension for slot length.

(i) *Summary.*—Individual slot size: 0.0625 in. width by 1.1 in. length. Longitudinal slot spacing: In every other corrugation root. Circumferential slot spacing: 3 rows at  $120^\circ$  intervals around tube.

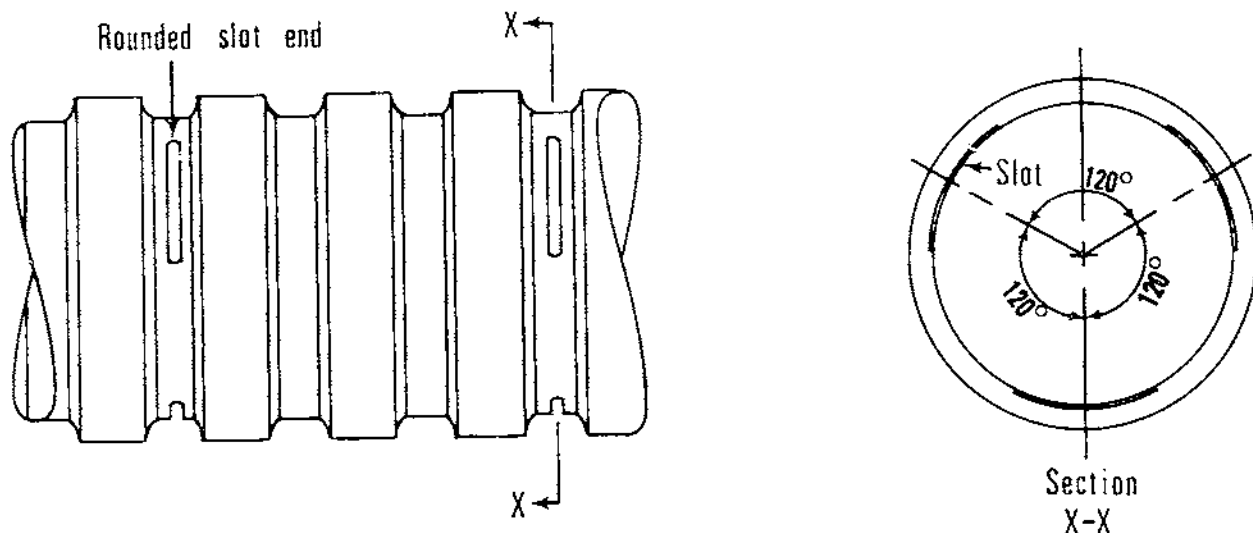


Figure 15.—Typical corrugated tube-wall slots for water entry.



## COMMENTS AND DISCUSSION

The author emphasizes that the results of the corrugated tube *design example* presented in this report should not be considered as a recommended design for a production draitube. Several factors may significantly change the selection of corrugation profile. For example, many HDPE plastic resins which might be used are not as rigid as the material considered in the design example, (that is,  $E = 95,000$  p.s.i.). A more complex corrugation profile with proper fillets to improve molding as the tube is extruded is needed for many types of plastic materials. In an actual design case, the corrugation pitch ( $P$ ) would preferably be selected as some multiple of the die-block length for the particular tube extrusion equipment to be used. Also, because of plastic shrinkage characteristics in extrusion operations, the corrugation die-block, or molds, will necessarily need to be larger than the tube size and corrugation profile desired. In addition, the minimum strength requirement assumed in the *design example* should probably be increased by as much as 30 to 50 percent to allow for hazards resulting from variable quality control of the manufactured plastic tubing and irregularities in the drain installation operation.

The accuracy of the design procedure was not verified or presented as a section of this report because actual drain tubing with the selected corrugation profile was not available for physical testing. Therefore, in retrospect, two corrugated plastic tubes from the author's collection were selected for analysis and testing to compare theoretical and physical test results of the tube strength-deflection. The details of these analyses and tests are presented in Appendix II. On the basis of the comparative results given in Appendix II (and in other analyses conducted by the author to theoretically predict a corrugated plastic tube's strength-deflection characteristics), it is concluded that the draitube design procedure outlined has an overall accuracy of approximately  $\pm 10$  percent. The theoretical prediction of a particular draitube's strength-deflection will be within about 10 percent of physical test results for an actual sample of the draitube—using the parallel-plate loading method. This is considered an acceptable design tolerance for such engineering work.

Although this report deals only with the linear range of tube deflection (as defined in fig. 1), many of the design principles presented can be used for designing into the nonlinear range of tube deflection. Design in the nonlinear range can be accomplished by utilizing the stress-strain data for the actual plastic material to be used (see fig. 3), and by defining an effective modulus of elasticity ( $E_{eff}$ ) which corresponds to the level of nonlinear stress ( $\sigma_{nl}$ ) and nonlinear strain ( $\epsilon_{nl}$ ) considered allowable; that is,  $E_{eff} \triangleq \frac{\sigma_{nl}}{\epsilon_{nl}}$ . (This is similar to the definition for the soil modulus ( $E'$ ) as shown in fig. 2.) With the use of this ( $E_{eff}$ ), the previously derived equations can be applied directly. An acceptable corrugation profile is one which will provide adequate tube strength (parallel-plate load) at the design deflection ( $\Delta y$  between parallel plates), and the critical tube-wall stress just equals the allowable limit of nonlinear stress ( $\sigma_{nl}$ ). Thus, the nonlinear design problem involves more trial-and-error than the linear design does; therefore, programming on a conventional digital computer, where trial-and-error iterative loops can be incorporated is advisable. However, procedure for the nonlinear design is beyond the scope of this report.

A final point of discussion is the proper method for comparing flexible draitubes of different diameters. For structural performance under either parallel-plate or soil-loading conditions, comparison on the basis of *percent* conduit deflection is the most meaningful. For example, if two draitubes of different diameters are to deflect the same amount on a diameter percentage basis under parallel-plate loading, then they must have the same conduit stiffness factor  $\left[ \frac{EI}{D_{NA}^3} \right]$  as shown below by writing equation 2 in the form:

$$\frac{W}{\Delta x} = \left( \frac{12 \cdot (2)^3}{0.136} \right) \left[ \frac{EI}{D_{NA}^3} \right]; \quad [63]$$

and by dividing both the numerator and denominator of the lefthand side by ( $D_{NA}$ ), equation 63 can be written in the proportionality form:

$$\frac{(W/D_{NA})}{(\Delta x/D_{NA})} \propto \left[ \frac{EI}{D_{NA}} \right]. \quad [64]$$

The proportionality expression equation 64 could have been derived from equation 4 for soil-loading conditions. However, further justification is needed for the corresponding equivalent loading term ( $W_c/D_{NA}$ ); that is, the relationship between the soil loads ( $W_{c_1}$  and  $W_{c_2}$ ) for two sizes of draitube being compared is

$$\frac{W_{c_1}}{D_{NA_1}} \approx \frac{W_{c_2}}{D_{NA_2}} \quad [65]$$

Inspection of equation 3 for computing soil load ( $W_c$ ) indicates that the corresponding soil load for another size tube might vary as ( $D_{NA}^2$ ) [or  $B_c^2$  as shown in equation 3]. However, more detailed study shows that the offsetting effect of ( $C_c$ ), or the load concentration factor, is such that relation 65 is much better for approximations when ( $D_{NA_1}$ ) and ( $D_{NA_2}$ ) do not differ greatly (for example, when comparing 4- and 5-inch tubing).

Thus, from equation 64, the following comparative formulae can be written to relate two different diameter draitubes so that equal performance can be expected, that is, the same percent deflection under either parallel-plate or soil loading:

$$W_2 = \left( \frac{D_{NA_2}}{D_{NA_1}} \right) W_1, \quad [66]$$

where ( $W$ ) is the parallel-plate load for convenience again;

$$\Delta v_2 = \left( \frac{D_{NA_2}}{D_{NA_1}} \right) \Delta v_1; \quad [67]$$

$$\left[ \frac{E_2 I_2}{D_{NA_2}^3} \right] = \left[ \frac{E_1 I_1}{D_{NA_1}^3} \right]; \quad [68]$$

or if the same plastic material is considered, that is,  $E_1 = E_2$ , then equation 68 can be written

$$I_2 = \left( \frac{D_{NA_2}}{D_{NA_1}} \right)^3 I_1 \quad [69]$$

## SELECTED REFERENCES

- (1) Anonymous.  
1966. MACHINE DESIGN. *Plastics Reference Issue*, pp. 77-78 (for HDPE, type III).
- (2) Boa, W.  
1963. DEVELOPMENTS OF A MACHINE FOR LAYING PLASTIC DRAINS. *Jour. Agr. Engin. Res.* 8: (3) 221-230.
- (3) Boyd, J. E., and Folk, S. B.  
1950. STRENGTH OF MATERIALS. Fifth ed., p. 360, McGraw Hill.
- (4) Cooper, A. W., and others.  
1957. STRAIN GAGE CELL MEASURES SOIL PRESSURE. *Agr. Engin.*: 38(4): 232-235, 246.
- (5) Ede, A. N.  
1963. NEW METHODS OF FIELD DRAINAGE. *Agriculture* 70: (2) 82-86.
- (6) ———  
1965. EUROPEAN STANDARDS AND SPECIFICATIONS FOR DRAINAGE MATERIALS. ASAE Paper No. 65-730. (c/o ASAE, St. Joseph, Mich. 49085.)
- (7) ———  
1965. NEW MATERIALS AND MACHINES FOR DRAINAGE. *Proc. ASAE Conf., Drainage for Efficient Crop Production*, pp. 58-61. (c/o ASAE, St. Joseph, Mich. 49085.)
- (8) FOUSS, J. L.  
1965. PLASTIC DRAINS AND THEIR INSTALLATION. *Proc. ASAE Conf., Drainage for Efficient Crop Production*, pp. 55-57. (c/o ASAE, St. Joseph, Mich. 49085.)
- (9) ———  
1968. CORRUGATED PLASTIC DRAINS PLOWED-IN AUTOMATICALLY. *Trans. of the ASAE* 11: (6) 804-808.
- (10) ——— and Donnan, W. W.  
1962. PLASTIC-LINED MOLE DRAINS. *Agr. Engin.* 43: (9) 512-515.
- (11) ——— and Reeve, R. C.  
1968. LASERS AND MOLES MAKE A PIPE DREAM COME TRUE. *Yearbook of Agriculture*, pp. 69-72.
- (12) Frevert, R. K., Schwab, G. O., Edminster, T. W., and Barnes, K. K.  
1966. SOIL AND WATER CONSERVATION ENGINEERING. Pp. 471-477 and 651-653, John Wiley & Sons.
- (13) Herndon, L. W.  
1969. USE OF CORRUGATED PLASTIC TUBING FOR SUB-SURFACE DRAINAGE. ASAE Paper No. NA 69-406. (c/o ASAE, St. Joseph, Mich. 49085.)
- (14) Lever, A. E., and Rhys, J.  
1962. THE PROPERTIES AND TESTING OF PLASTIC MATERIALS. 2d ed., pp. 20, and 220-226, When Pub. Co., New York.
- (15) Myers, V. I., and Rektorik, R. J.  
1967. DEFLECTION TESTS AND TRENCH CONDITIONS FOR PLASTIC DRAIN PIPE. *Trans. of the ASAE* 10: (4) 454-457.

- (16) Rektorik, R. J., and Myers, V. I.  
1967. POLYETHYLENE DRAINAGE PIPE INSTALLATION TECHNIQUES AND FIELD PERFORMANCE. Trans. of the ASAE 10: (4) 458-461.
- (17) Schwab, C. O.  
1955. PLASTIC TUBING FOR SUBSURFACE DRAINAGE. Agr. Engin. 36: (2) 86-89, 92.
- (18) ——— DeBoer, D. W., and Johnson, H. P.  
1969. EFFECT OF OPENINGS ON DESIGN OF SUBSURFACE DRAINS. Jour. Irrigation and Drainage Div., American Society of Civil Engineers, Vol. 95, No. 1R1, pp. 199-209, Proceedings Paper 6480.
- (19) Van Someren, C. L.  
1964. THE USE OF PLASTIC DRAINAGE PIPES IN THE NETHERLANDS. (Translation from Cultuurtechnik 1, 2, and 3.) Government Service for Land and Water use, Maleibaan 21, Utrecht, The Netherlands.
- (20) Soribe, F. I.  
1969. LOAD-DEFLECTION CHARACTERISTICS OF CORRUGATED PLASTIC DRAINAGE TUBING. M.S. thesis, The Ohio State University, Agr. Engin. Dept. (Also see ASAE Paper No. 70-210.)
- (21) Spangler, M. G.  
1960. SOIL ENGINEERING. 2d ed., p. 433, International Textbook Co., Scranton, Pa.
- (22) U.S. Department of Agriculture  
1969. ENGINEERING STANDARDS FOR SUBSURFACE DRAINAGE. U.S. Soil Conservation Service No. 606-1, August 1969.
- (23) Watkins, R. K. and Spangler, M. G.  
1958. SOME CHARACTERISTICS OF THE MODULUS OF PASSIVE RESISTANCE OF SOIL: A STUDY IN SIMILITUDE. Highway Research Board Proceedings, v. 37, pp. 576-583.

## APPENDIX I

The following are example tests to empirically determine the modulus of elasticity ( $E$ ) for HDPE plastic material.

Two strip samples of plastic material described in figures 16 and 17 were tested in accordance with the method shown in figure 3, page 9; the tabulated results are given in tables 5 and 6, and are graphed in figure 18.

The graphical method of determining the value for the modulus of elasticity ( $E$ ) is shown in figure 18. Note that, for the *design example*, the linear range for stress and strain was assumed somewhat larger than indicated by the data points in order to use rounded numbers in the design computations.

Sample No. I of HDPE plastic was weighed in air and then in gasoline (plastic will float in water) in order to empirically determine its specific gravity ( $\rho_p$ ); the computed method is shown below using actual measured weights:

	Thickness (in.)	Width (in.)
	0.0519	0.2046
	0.0539	0.2033
	0.0553	0.2061
	0.0533	0.2066
(Avg.)	0.0536	0.2051

Avg. X-sect. area of plastic strip =

$$0.0536 \times 0.2051 = 0.011 \text{ in.}^2$$

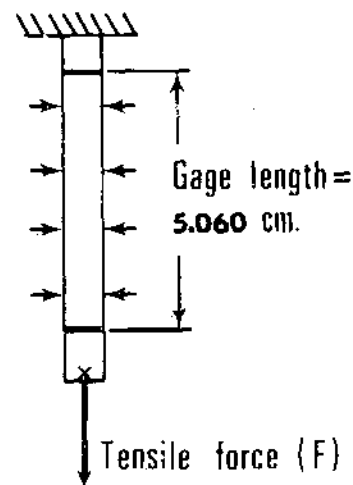


Figure 16. — Sample I: Specimen (cut from ridge of corrugated tube) measured to determine cross-sectional area.

Thickness (in.)	Width (in.)
0.0430	0.2205
0.0450	0.2141
0.0468	0.2133
<u>0.0500</u>	<u>0.2104</u>
(Avg.) 0.0462	0.2148

Avg. X-section area of plastic strip =

$$0.0462 \times 0.2148 = 0.0099 \text{ in.}^2$$

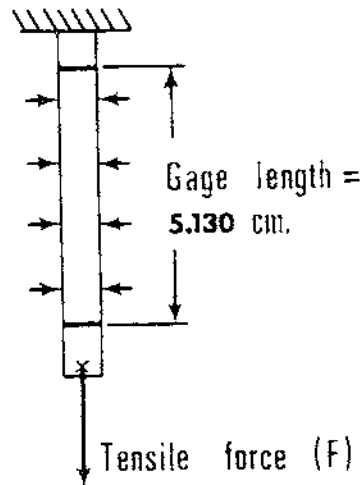


Figure 17. — Sample II: Specimen (cut from ridge of corrugated tube) measured to determine cross-sectional area.

TABLE 5. — Sample I: Example tension test (per method in fig. 3) of HDPE plastic strip to obtain stress ( $\sigma$ ) and strain ( $\epsilon$ ) data  
(Original test, October 1968; data copied December 1969)

Lead increment.	Time load increment applied	Time of measuring elongation <sup>1</sup>	Total tensile force <sup>2</sup>	Tensile stress ( $\sigma$ )	Cathetometer reading		Gage length elong.	Unit strain ( $\epsilon$ )	Remarks
					Top mark	Bottom mark			
No.	Hr., min. (p.m.)	Hr., min. (p.m.)	lb.	p.s.i.	cm.	cm.	cm.	Percent	
		(Start/Stop)	(Gage length = 5.060 cm.)						
1.....	2:35	2:38/2:42	0.30	27.3	82.960	77.900	0.00+	=0	Initial
2.....	2:42	2:45/2:47	1.06	96.4	82.945	77.880	0.005	0.099	load =
3.....	2:47	2:50/2:52	2.06	187.3	82.915	77.845	0.010	0.198	clamp +
4.....	2:52	2:55/2:58	3.06	278.2	82.900	77.825	0.015	0.296	hook
5.....	2:58	3:01/3:07	4.06	369.1	82.885	77.805	0.020	0.395	weights.
6.....	3:07	3:10/3:15	5.06	460.0	82.860	77.775	0.025	0.494	
7.....	3:15	3:18/3:22	6.06	550.9	82.840	77.750	0.030	0.593	
8.....	3:22	3:25/3:28	7.06	641.8	82.815	77.720	0.035	0.692	Air temp.
9.....	3:28	3:31/3:34	8.06	732.7	82.795	77.690	0.045	0.889	= 75°-80° F.
10.....	3:34	3:37/3:40	9.06	823.6	82.780	77.665	0.055	1.087	
11.....	3:40	3:43/3:46	10.06	914.5	82.760	77.635	0.065	1.285	
12.....	3:46	3:49/3:52	11.06	1005.4	82.735	77.600	0.075	1.482	
13.....	3:52	3:55/4:00	12.06	1096.4	82.695	77.550	0.085	1.680	Final load.
14.....	4:00	4:03/4:06	13.06	1187.3	82.465	77.310	0.095	1.878	

<sup>1</sup> Elongation is measured after load increment has been applied  $\approx$  3 min.

<sup>2</sup> Applied in increments of 1.00 lb. @ 5 to 8 minute time intervals (see footnote 1).

TABLE 6.—Sample II: Example tension test (per method in fig. 3) of HDPE plastic strip to obtain stress ( $\sigma$ ) and strain ( $\epsilon$ ) data

(Original test, October 1968; data copied December 1969.)

Local incom.	Time load increment applied	Time of measuring elongation <sup>1</sup>	Total tensile force <sup>2</sup>	Tensile stress ( $\sigma$ )	Cathetometer reading		Gage length elong.	Unit strain ( $\epsilon$ )	Remarks
					Top mark	Bottom mark			
No.	Hr., min. (a.m.)	Hr., min. (a.m.)	lb.	p.s.i.	Cm.	Cm.	Cm.	Percent	
		(Start/Stop)			(Gage lgth. = 5.130 cm.)				
1.....	8:50	8:53/ 8:56	0.30	30.2	83.700	78.570	0.00+	≈ 0	Initial
2.....	8:56	8:59/ 9:03	1.06	106.8	83.660	78.530	0.00	0.000	load=
3.....	9:03	9:06/ 9:10	2.06	207.6	83.640	78.505	0.005	0.097	clamp+
4.....	9:10	9:13/ 9:18	3.06	308.4	83.620	78.480	0.010	0.195	hook
5.....	9:18	9:22/ 9:25	4.06	409.2	83.585	78.440	0.015	0.292	weights.
6.....	9:25	9:28/ 9:30	5.06	509.9	83.560	78.410	0.020	0.390	
7.....	9:30	9:33/ 9:38	6.06	610.7	83.540	78.380	0.030	0.585	Air temp.
8.....	9:38	9:41/ 9:44	7.06	711.5	83.515	78.350	0.035	0.682	≈ 75° F.
9.....	9:44	9:47/ 9:50	8.06	812.3	83.485	78.310	0.045	0.877	
10.....	9:50	9:53/ 9:55	9.06	913.1	83.465	78.285	0.050	0.975	
11.....	9:55	9:58/10:00	10.06	1013.8	83.430	78.240	0.060	1.170	
12.....	10:02	10:05/10:08	11.06	1114.6	83.405	78.205	0.070	1.365	
13.....	10:08	10:11/10:14	12.06	1215.4	83.370	78.160	0.080	1.560	
14.....	10:14	10:17/10:20	13.06	1316.2	83.340	78.115	0.095	1.852	Final load.

<sup>1</sup> Elongation if measured after load increment has been applied  $\geq$  3 min.<sup>2</sup> Applied in increments of 1.00 lb. @ 6- to 8-minute time intervals.

$v_p \triangleq$  measured volume of plastic from the tube specimen

$$= \frac{W_{air} - W_{gasoline}}{\gamma_{gasoline}} = \frac{(44.276 - 9.572) \text{ gm.}}{0.752 \text{ gm./cm.}^3}$$

$$v_p = 46.149 \text{ cm.}^3$$

$\gamma_p \triangleq$  density of plastic in the tube specimen

$$= \frac{W_{air}}{v_p} = \frac{44.276 \text{ gm.}}{46.149 \text{ cm.}^3} = 0.959 \text{ gm./cm.}^3,$$

therefore,

$$\rho_p = 0.959 \text{ (empirically)}$$

## APPENDIX II

The following are example structural analyses of two corrugated plastic drainage tubes to verify design procedure presented in this report.

### Analysis Example 1

**Tube description.**—HDPE plastic (same plastic material as tested in Appendix I for  $E$ -value).

Sample length: 6 inches, w/o water entry perforations.

Sample weight: Approx. 0.25 lb./lin. ft. (specific data for this sample missing).

Wall thickness variation; see sketches in figure 19. Note that ( $T_w$ ) is thinner than ( $T_o$ ), which indicates a poor quality extrusion; this was probably caused by the completely vertical webs in the square-wave corrugation profile as sketched in figure 20. This special corrugation was made for research purposes only, however, and would not be recommended for production tubing.

**Evaluation by parallel-plate testing.**—The data in table 7 were obtained by testing the tube sample in accordance with the method shown in figure 1, page 3.

The graph in figure 21 shows parallel-plate test data. Note the advantage of plotting the data to determine any nonlinearities in the data points at the origin.

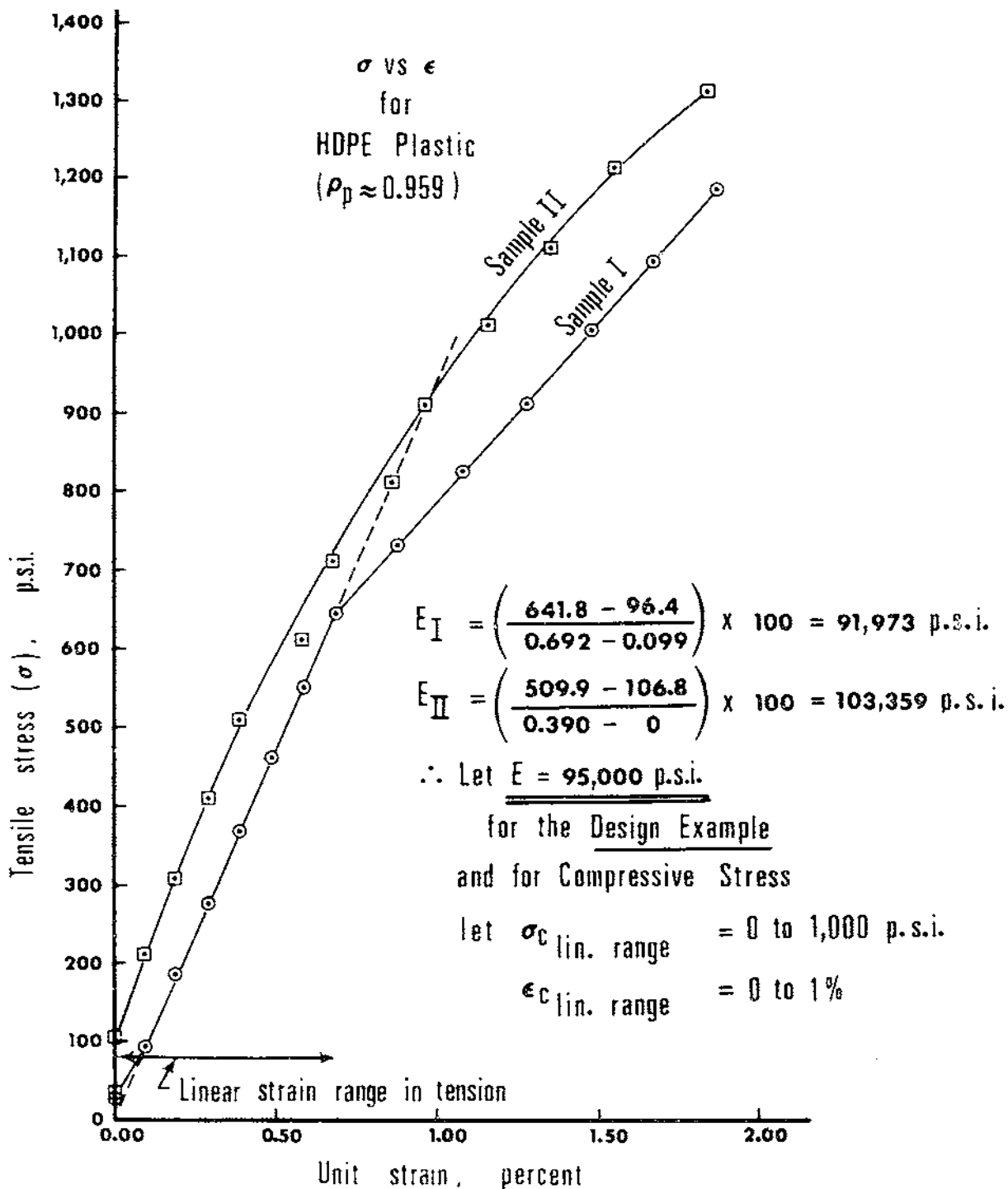


Figure 18.—Example graph of stress ( $\sigma$ ) versus strain ( $\epsilon$ ) for HDPE plastic tested in tension.

**Analytical evaluation.**—Depth of corrugation: and

$$H = 0.12 - \frac{0.036}{2} + \frac{0.049}{2} = \mathbf{0.1265 \text{ inch} = H}$$

$$(H - k) = (0.1265 - 0.0729)$$

$$= \mathbf{0.0536 \text{ inch} = (H - k)}$$

Location of  $NA$  of corrugation profile is determined as follows (see fig. 20):  $T_i L_i (H - k) \approx T_o L_o k$ , if the shift of the  $NA$  is neglected for the corrugation webs. Since  $L_i \approx L_o$ , the above can be written as

$$T_i (H - k) = T_o k$$

Thus,  $NA \neq \mathcal{L}$  for this example corrugation profile, and therefore, the shift in the  $NA$  will need to be taken into account in the analysis below.

Computation for  $D_{NA}$

$$D_{NA} = D_o - T_o - 2k = 3.12 - 0.036 - (2)(0.0729)$$

$$= \mathbf{2.938 \text{ in.} = D_{NA}}$$

or

$$k = \frac{T_i H}{(T_i + T_o)} = \frac{(0.049)(0.1265)}{(0.049 + 0.036)}$$

$$= \mathbf{0.0729 \text{ inch} = k}$$

The moment-of-inertia ( $I$ ) for the corrugated tube wall is computed as follows

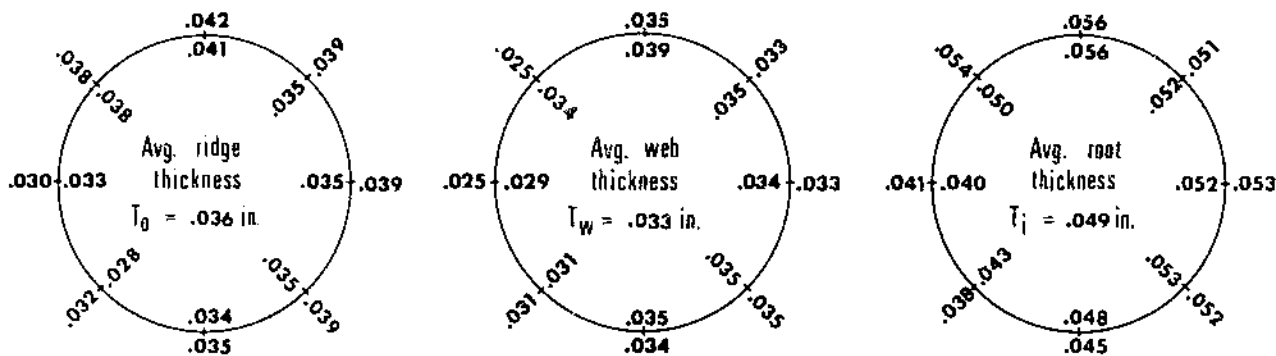
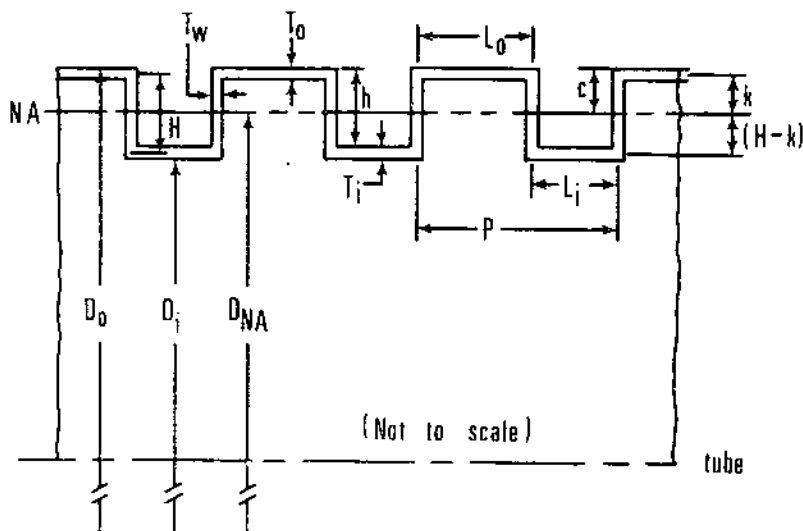


Figure 19.—Example 1: Wall thickness variation (measured at both ends of the sample).



Dimensions by measurement:

$$D_o = 3.12 \text{ in.}$$

$$D_i = 2.84 \text{ in.}$$

$$T_o = 0.036 \text{ in.}$$

$$T_i = 0.033 \text{ in.}$$

$$T_j = 0.049 \text{ in.}$$

$$L_o = 0.22 \text{ in.}$$

$$L_i = 0.22 \text{ in.}$$

$$P = 0.44 \text{ in.}$$

$$h = 0.12 \text{ in.}$$

Average from figure 19

Note:  $L_i = L_o$

Figure 20.—Example 1: Corrugation profile.

$$I = \frac{1}{P} \left[ \frac{2T_w H^3}{12} + 0^* + \frac{L_o T_n^3}{12} + L_o T_o k^2 + \frac{L_i T_i^3}{12} + L_i T_i (H - k)^2 \right]$$

\* (because small effect on shift in  $N_A$  on webs of corrugation)

$$= \frac{1}{0.44} \left[ \frac{(2)(0.033)(0.1265)^3}{12} + 0^* + \frac{(0.22)(0.036)^3}{12} + \frac{(0.22)(0.049)^3}{12} + (0.22)(0.049)(0.0536)^2 \right]$$

$$I = 0.000191 \frac{\text{in.}^4}{\text{lin. in.}}$$

Parallel-plate load-deflection resistance is computed as follows:

TABLE 7.—Example 1: Evaluation by parallel-plate testing

(Test conducted February 8, 1968)

[#] Parallel-plate load	[ $\Delta y$ ] Tube-deflection <sup>1</sup>
lb./ft.	inch
0	0.000
5	.016
10	.027
15	.041
20	.053
25	.065
30	.078
35	.090
40	.102
45	.115
50	.127
55	.141
60	.153
65	.168
70	.184
75	.196
80	.213
85	.227
90	.242
95	.256
100	.275
105	.289

<sup>1</sup> Tube deflection was recorded at approximately 1- to 2-minute intervals after each load increment.

From Appendix I,  $E = 95,000$  p.s.i. (since the same plastic is involved). Based on  $W$  vs  $\Delta y$  graph in figure 21, let  $\Delta y = 0.125$  in., which is approximately at the linear limit of deflection. Thus,

$$W = \frac{12 EI \Delta y}{0.149 \left( \frac{D_{NA}}{2} \right)^3} = \frac{(12)(95,000)(0.000191)(0.125)}{(0.149)(2.938/2)^3} = 57.6 \text{ lb./ft.}$$

That is,  $W = 57.6$  lb./ft. @  $\Delta y = 0.125$  in. (Theoretically.)

Comparison of actual and theoretical tube strength values:

$$\frac{W_{theor.}}{W_{actual}} \text{ ratio} = \frac{57.6}{51} = 1.13.$$

That is, the theoretical prediction of the sample tube's parallel-plate strength for  $\Delta y = 0.125$  in. is within about 13 percent of the actual measured value. The significant variation in the tube-wall thickness around the tube circumference may be the major contributing factor to this difference between the actual and theoretical values (see figure 20); however, this accuracy in predicting the tube's strength, up to the linear limit of deflection, is considered acceptable.

The tube's unit weight by computation is estimated by equation 25.

$$A_w \approx \frac{1}{0.44} [(0.22)(0.036) + (0.22)(0.049) + (2)(0.033)(0.1265)]$$

$$A_w = 0.0615 \frac{\text{in.}^2}{\text{lin. in.}} \text{ (one side).}$$

From equations 29, for  $\rho_p = 0.959$  (from Appendix I); that is, equation 30,

$$w = (1.305)(2.938)(0.0615) = 0.236 \text{ lb./lin. ft.} = w$$



(by computation) and is within  $\frac{0.236}{0.25} \times 100 = 94.4$  percent, or 5.6 percent of the measured weight.

Computation for tube-wall stress due to parallel-plate loading:

To compare the computed values for tube-wall stress with the results of the parallel-plate test for the tube sample as graphed in figure 21, ( $W$  vs  $\Delta y$ ) and the ( $\sigma$  vs  $\epsilon$ ) graph in figure 18; let  $\Delta y = 0.125$  in., which should be approximately the proportional limit deflection, and  $W = 51$  lb./ft. ( $W$  and  $\Delta y$  values read from graph in figure 21).

Since  $k$  is larger than  $H-k$  for this sample tube (that is, the  $NA \neq E$  of the corrugation profile), equation 37 becomes

$$C = k + \frac{T_e}{2} = 0.0729 + \frac{0.036}{2}$$

$$C = 0.0909 \text{ in.}$$

When  $\sigma_B$  due to  $\Delta y = 0.125$  in. and  $\sigma_c$  due to  $W = 51$  lb./ft., is determined and when it is recalled that  $\Delta x = \Delta y/1.09$  for parallel-plate loading, equation 38 for this example analysis becomes

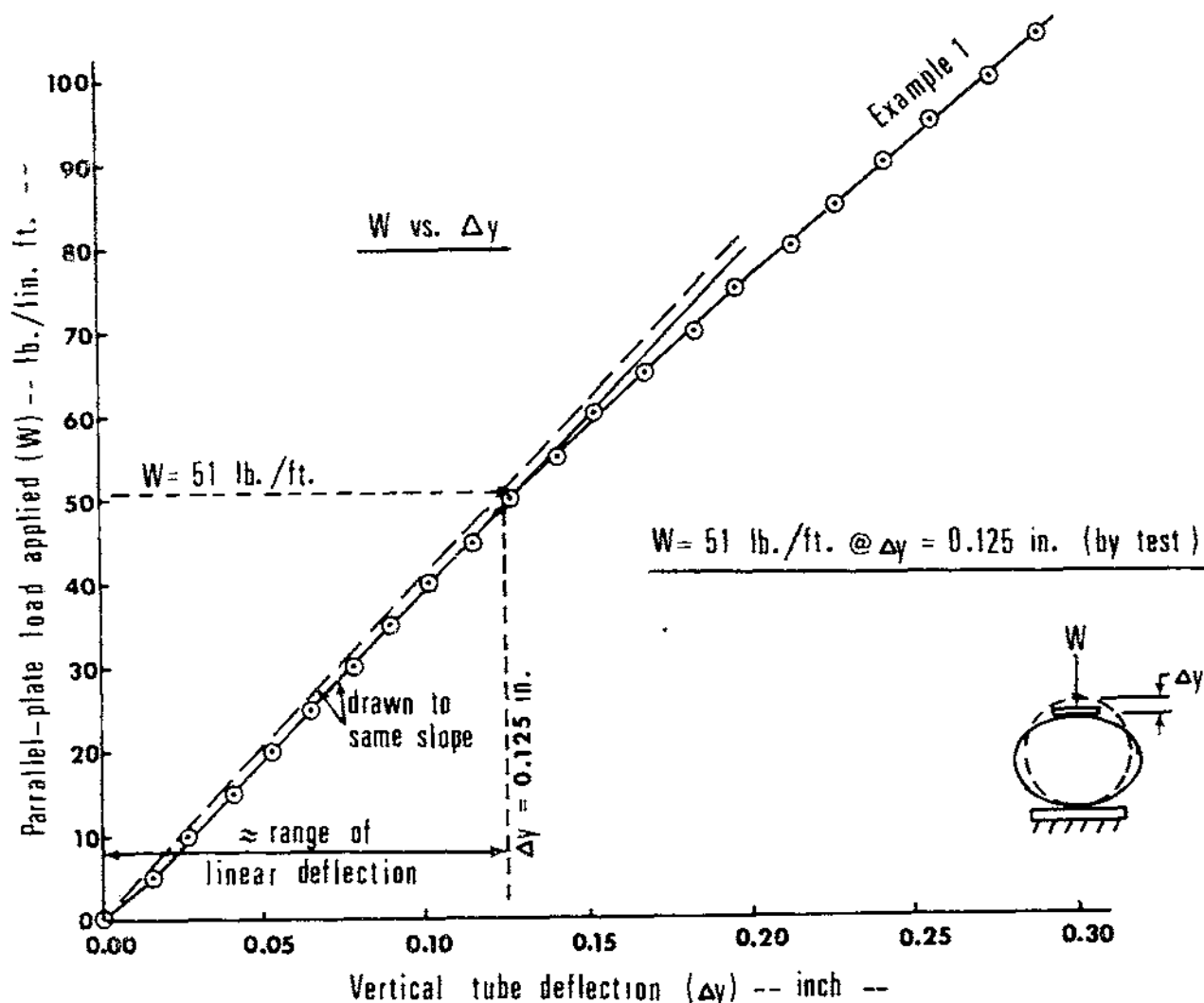


Figure 21.—Example 1: Parallel-plate load versus vertical tube deflection for corrugated plastic drain tube. [ $D_{NA} = 2.938$  in.;  $D_o = 3.12$  in.;  $D_i = 2.84$  in.; HDPE;  $E = 95,000$  p.s.i. (from Appendix I);  $l = 0.000191$  in./in. (from part 2 of this example)].

$$\sigma_B = 5.32 \left[ \frac{EC}{D_{NA}^2} \right] \frac{\Delta y}{1.09}$$

$$= (5.32) \left[ \frac{(95,000)(0.0909)}{(2.938)^2} \right] \left( \frac{0.125}{1.09} \right)$$

$$\sigma_B = 610 \text{ p.s.i.}$$

And, equation 31, for the case of parallel-plate load  $W$ , applied becomes

$$\sigma_c = \frac{W}{24A_w} = \frac{51}{(24)(0.0615)} = 35 \text{ p.s.i.}$$

$$\sigma_c = 35 \text{ p.s.i.}$$

Thus,  $\sigma_{TC} = \sigma_B + \sigma_c = 610 + 35 = 645 \text{ p.s.i.}$   $\sigma_{TC} = 645 \text{ p.s.i.}$  (for parallel-plate load  $W = 51 \text{ lb./ft.}$  and  $\Delta y = 0.125 \text{ in.}$ )

Inspection of the ( $\sigma$  vs  $\epsilon$ ) graph for this HDPE plastic material given in figure 18, Sample 1, indicates that nonlinear strain would be expected to begin at about the stress of  $650 \text{ p.s.i.}$ , which closely approximates the computed value for  $\sigma_{TC}$  above, which in turn was computed by the use of parallel-plate test data. Thus, the analysis procedure is shown to be valid and accurate.

### Analysis Example 2<sup>18</sup>

**Tube description.**—HDPE plastic;  $\rho_p = 0.954$  (sp. gr. by weighing in gasoline).

<sup>18</sup>All measurements, laboratory tests, and analyses for this example were conducted or made by the author, personally.

Sample length: 4 inches; 3 rows water entry slots @ 120° apart and in every third corrugation.  
Sample weight: 43.94 gm.; 0.290 lb./lin. ft.

Wall thickness variation; see figure 22.

Corrugation profile: See sketch of approximate corrugation profile in figure 23.

**Evaluation by parallel-plate testing.**—The data in table 8 were obtained by testing the tube sample with the parallel-plate device sketched in figure 24.

See graph in figure 25 of parallel-plate test data; note the advantage of plotting the data to determine any nonlinearities in the data points at the origin.

**Analytical Evaluation.**—Structurally equivalent corrugation profile (for analysis purposes) is shown in figure 26. When this figure is referenced, the physical parameters of the corrugation profile are:

$$\text{Depth of corrugation: } H = 0.28 - \frac{0.029}{2} - \frac{0.051}{2} = 0.24 = H.$$

Location of  $NA$  of corrugation profile (based on equivalent profile)

$$T_o L_o k \approx T_i L_i (H - k)$$

$$k = \frac{T_i L_i H}{(T_o L_o + T_i L_i)} = \frac{(0.051)(0.15)(0.24)}{(0.029)(0.25) + (0.051)(0.15)}$$

$$k = 0.123 \text{ inch.}$$

$(H - k) = 0.117 \text{ inch}$ ; thus,  $NA \neq E$  of the corrugation profile.

Computation for  $NA$  tube diameter:

$$D_{NA} = 4.00 + 0.51 + (2)(0.117) = 4.285 \text{ inch} = D_{NA}$$

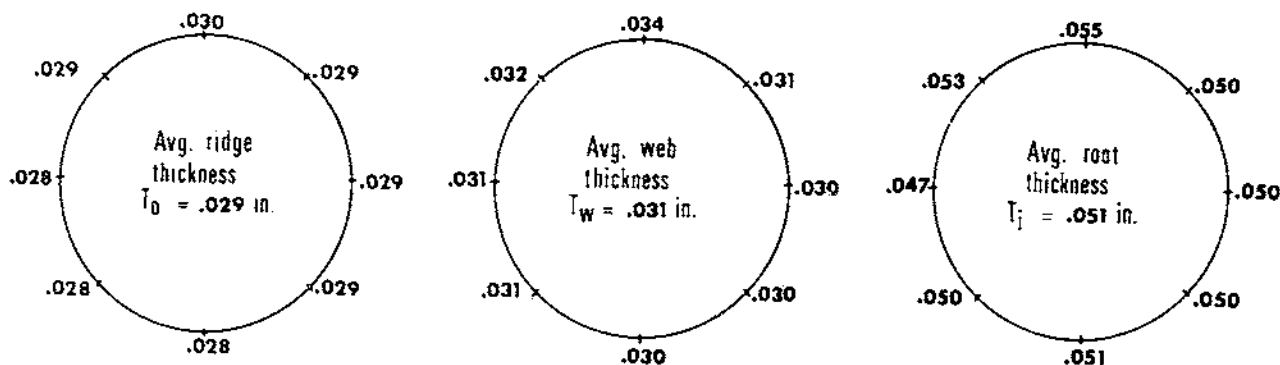


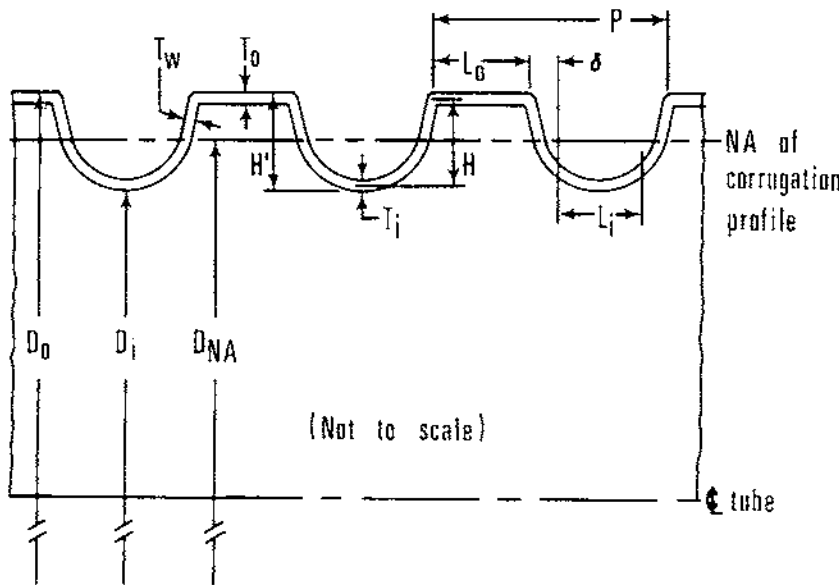
Figure 22. — Example 2: Wall thickness variation.

TABLE 8.—*Example 2: Evaluation by parallel-plate testing*

(Sample length=4 in., laboratory air temp. ≈ 75°F., date 3/13/69)

Time	Platform scale reading	Accumulated weight (M) <sup>1</sup>	Load on sample (3/4 × accum.)	Unit load <i>W</i>	Accumulated tube deflection <sup>2</sup> Δ <i>y</i>
<i>Hr., min.</i>	<i>Lb.</i>	<i>Lb.</i>	<i>Lb.</i>	<i>Lb./ft.</i>	<i>Inch</i>
15:50	<sup>3</sup> 51.5	0	0	0	0
15:50	52.5	1.0	0.75	2.25	0.012
15:53	53.5	2.0	1.50	4.50	.022
15:55	55.0	3.5	2.63	7.88	.035
15:57	56.0	4.5	3.38	10.13	.045
15:59	57.0	5.5	4.13	12.38	.055
16:01	58.0	6.5	4.88	14.63	.064
16:03	59.0	7.5	5.63	16.88	.073
16:06	60.0	8.5	6.38	19.13	.082
16:08	61.5	10.0	7.50	22.50	.095
16:10	62.5	11.0	8.25	24.75	.105
16:12	63.5	12.0	9.00	27.00	.115
16:15	64.5	13.0	9.75	29.25	.126
16:18	65.5	14.0	10.50	31.50	.138
16:20	66.5	15.0	11.25	33.75	.149
16:22	67.5	16.0	12.00	36.00	.162
16:25	69.0	17.5	13.13	39.38	.173
16:27	70.0	18.5	13.88	41.63	.185
16:30	71.0	19.5	14.63	43.88	.201
16:32	72.5	21.0	15.75	47.25	.218
16:35	73.5	<sup>4</sup> 22.0	16.60	49.50	.233
<sup>5</sup> 16:40	51.5	.....	.....	.....	.....
16:45	51.5	0	0	0	.060
16:47	51.5	0	0	0	.050
<sup>6</sup> 17:35	51.5	0	0	0	.020
08:00	51.5	0	0	0	<sup>7</sup> .003

<sup>1</sup> Increased the load by adding water into a bucket (*M<sub>H<sub>2</sub>O</sub>*); loads applied at 2- to 3-minute intervals.<sup>2</sup> Accumulated tube deflection (Δ*y*) measured with Ames Dial.<sup>3</sup> Tare weight on platform scale was 51.5 lb.<sup>4</sup> Final loading increment.<sup>5</sup> Load removed gently by siphoning water from bucket.<sup>6</sup> Fourteen hours had elapsed between the last two readings (3/14/69).<sup>7</sup> Tube sample had essentially returned to original shape.



Dimensions by measurement :

$$D_0 = 4.56 \text{ in.}$$

$$D_i = 4.00 \text{ in.}$$

$$T_0 = 0.029 \text{ in.}$$

$$T_w = 0.031 \text{ in.}$$

$$T_i = 0.051 \text{ in.}$$

$$P = 0.50 \text{ in.}$$

$$L_0 = 0.25 \text{ in.}$$

$$L_i = 0.15 \text{ in.}$$

$$\delta = 0.05 \text{ in.}$$

$$H' = 0.28 \text{ in.}$$

Average from figure 22.

Figure 23. — Example 2: Corrugation profile.

Computed moment-of-inertia ( $I$ ) for the corrugated tube-wall is:

$$I = \frac{1}{P} \left[ \frac{2T_w H^3}{12} + 0 + \frac{L_0 T_0^3}{12} \right]$$

\*(small effect due to shift in NA on webs)

$$+ L_0 T_0 k^2 + \frac{L_i T_i^3}{12} + L_i T_i (H - k)^2$$

$$= \frac{1}{0.5} \left[ \frac{(2)(0.031)(0.24)^3}{12} + \frac{(0.25)(0.029)^3}{12} \right]$$

$$+ (0.25)(0.029)(0.123)^2 + \frac{(0.15)(0.051)^3}{12}$$

$$+ (0.15)(0.051)(0.117)^2$$

$$I = 0.000576 \frac{\text{in.}^4}{\text{lin. in.}}$$

Value of modulus of elasticity ( $E$ ) is estimated as follows:

For HDPE:  $\rho_p = 0.954$  (actual  $\sigma$  vs  $\epsilon$  data not available). Therefore, from the discussion in step 5, page, 6, where  $E_{\rho_p=0.94} \approx 50,000$  p.s.i. and

$E_{\rho_p=0.96} \approx 140,000$  p.s.i., and if a linear relationship between  $E$  and  $\rho_p$  for HDPE is assumed, the value for  $E_{\rho_p=0.954}$  can be obtained by interpolation as

$$E_{\rho_p=0.954} \approx 50,000 + \frac{(140,000 - 50,000)}{(0.96 - 0.94)}$$

$$\times (0.954 - 0.94) = 50,000 + 63,000$$

or

$$E_{\rho_p=0.954} \approx 113,000 \text{ p.s.i.}$$

But, as discussed in step 5,  $E_{design}$  should be taken as about one-half to two-thirds of this value. Therefore, for analysis purposes here, set  $E_{design}$  or  $E_{analysis} = \frac{1}{2} (E_{\rho_p=0.954}) \approx E (\frac{1}{2} \text{ used because a more conservative estimate or minimum value of tube strength will be predicted) or}$

$$E \approx 56,000 \text{ p.s.i.}$$

Computation for parallel-plate, load-deflection resistance: Letting  $\Delta y = 0.125$  inch, so that direct comparison with the test results shown in figure 25 can be made,

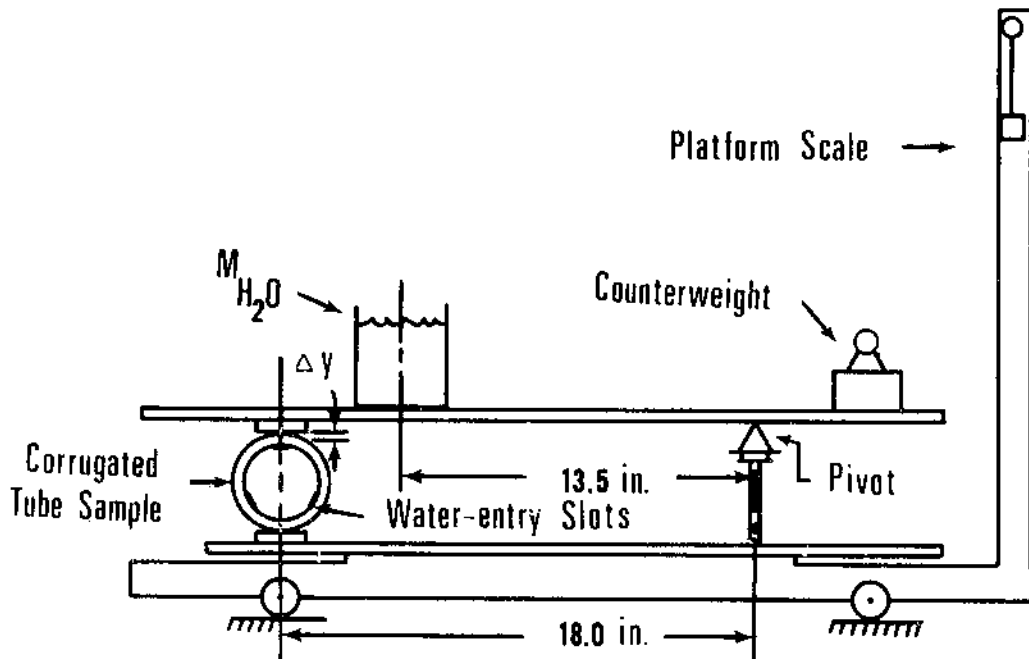


Figure 24. — Laboratory parallel-plate, load-deflection test device.

$$W = \frac{12EI\Delta y}{0.149(D_{NA}/2)^3} = \frac{(12)(56,000)(0.000576)(0.125)}{(0.149)(4.285/2)^3} = 33 \text{ lb./ft.};$$

that is, **W = 33 lb./ft. @ Δy = 0.125 inch (theoretically, with estimated E-value).**

Comparison of actual and theoretical tube strength (*W*) values:

$$\frac{W_{theor.}}{W_{actual}} - \text{ratio} = \frac{33}{30} = 1.10.$$

That is, the *theoretical prediction* is only 10 percent higher than the actual tube strength Δy = 0.125 in., which is approximately the linear limit of deflection (see fig. 25).

Illustration of alternative method for determining an experimental value for *E* from parallel-plate test data; that is, from  $W_{actual} = 30 \text{ lb./ft. @ } \Delta y = 0.125 \text{ in.}$

$$\text{Then, } E_{calc.} = \frac{0.149 \left(\frac{D_{NA}}{2}\right) W}{12 I \Delta y} = \frac{(0.149) \left(\frac{4.285}{2}\right)^3 (30)}{(12)(0.000576)(0.125)}$$

$$E_{calc.} \approx 51,000 \text{ p.s.i.}$$

So, in terms of the actual parallel-plate test data, and the assumption that (*I*) was computed as accurately as possible, the modulus of elasticity (*E*) for the HDPE used is approximately 51,000 p.s.i., which is close to that estimated at 56,000 p.s.i. by the rule-of-thumb method.

Estimation of the tube's unit weight by computation: ( $\rho_p = 0.954$ , by measurement). If the equivalent corrugation profile for simplicity (although it is not as accurate) is used,

$$A_w \approx \frac{1}{P} [L_o T_o + L_i T_i + 2T_w H]$$

$$= \frac{1}{0.5} [(0.25)(0.029) + (0.15)(0.051) + (2)(0.031)(0.24)]$$

$A_w = 0.05956 \text{ in./lin. in.}$  (on one side of the tube)  
 $w = 12\pi D_{NA} A_w \rho_p \gamma_{H_2O} = (1.361)(0.05956)(0.954)(4.285)$   
 $w = 0.33 \text{ lb./ft.}$  (by computation), which is

$$\frac{0.33}{0.29} = 1.14$$

about 14 percent heavier than the actual measured weight 0.29 lb./ft.

Unit strain ( $\epsilon$ ) in the tube wall at linear limit of tube deflection is calculated as follows:

From the graph of ( $W$  vs  $\Delta y$ ) in figure 25, the maximum tube deflection for which linear strain would still be governing, appears to be at  $\Delta y \approx 0.125$  in., where  $W = 30$  lb./ft. Since  $k > (H - k)$ ,

$$C = k + \frac{T_0}{2} = 0.123 + \frac{0.029}{2}$$

$$C = 0.138 \text{ in.}$$

Thus, equation 38 for this example becomes,

$$\sigma_B = 5.32 \left[ \frac{EC}{D_{NS}^2} \right] \frac{\Delta y}{1.09} = \frac{(5.32)(56,000)(0.138)(0.125)}{(4.285)^2 (1.09)}$$

$$\sigma_B = 257 \text{ p.s.i.}$$

And for the applied parallel-plate load  $W = 30$  lb./ft.,

$$\sigma_c = \frac{W}{24A_w} = \frac{30}{(24)(0.0596)} \approx 21 \text{ p.s.i.} = \sigma_c$$

Thus,  $\sigma_{TC} = \sigma_B + \sigma_c = 257 + 21 = 278 \text{ p.s.i.} = \sigma_{TC}$

And now, from the definition of unit strain,

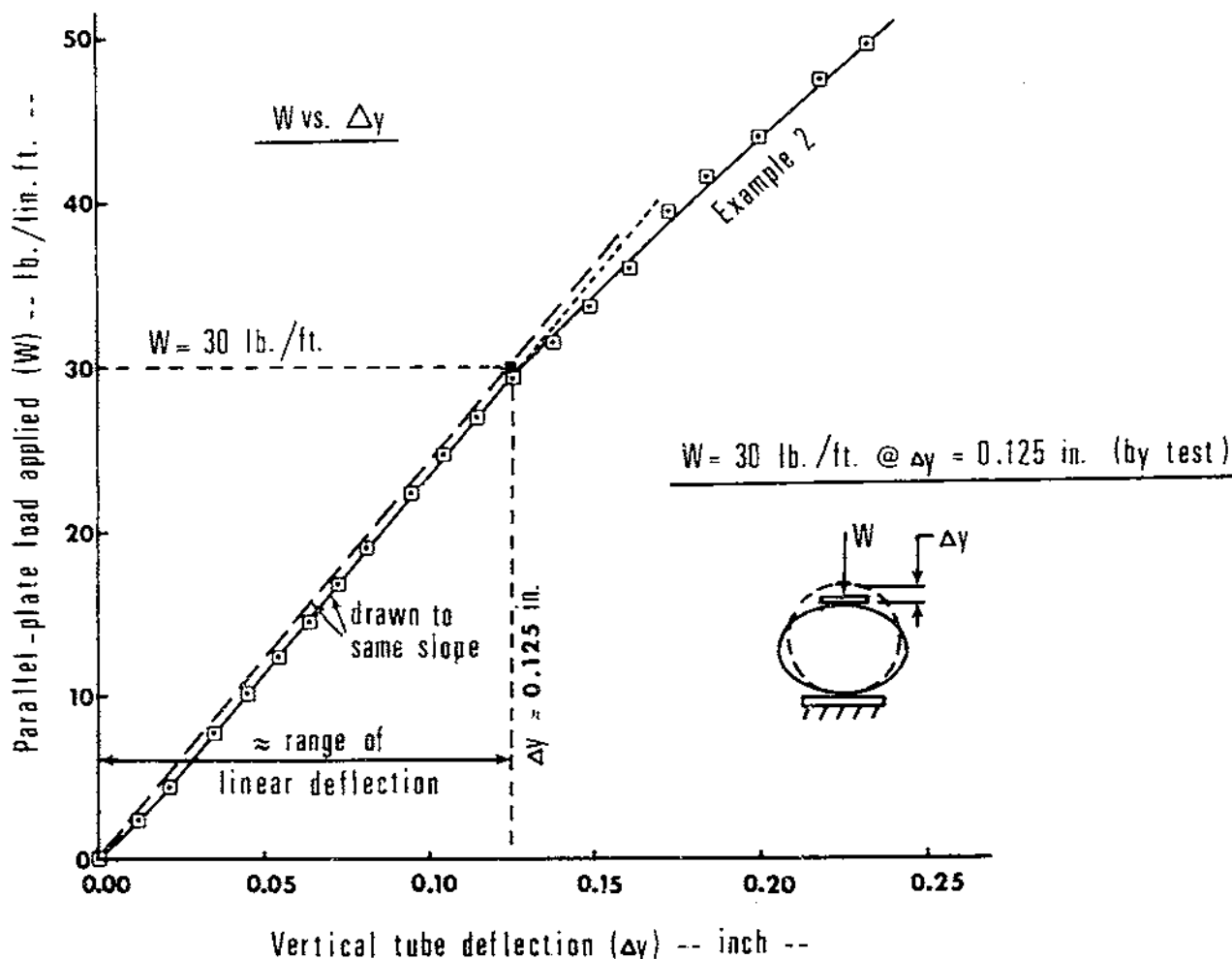


Figure 25. — Example 2: Parallel-plate load versus vertical tube deflection for corrugated plastic drain tube. [ $D_o = 4.56$  in.;  $d_i = 4.00$  in., HDPE;  $\rho_p = 0.954$ .]

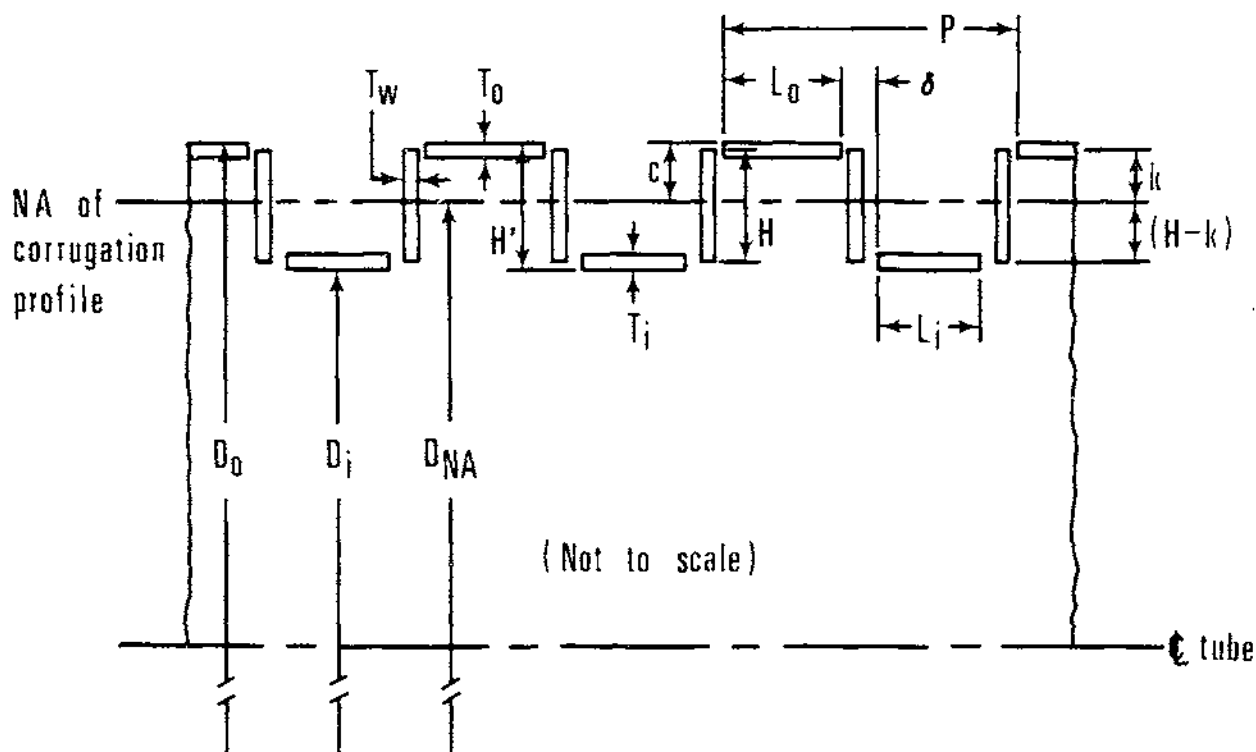


Figure 26.—Example 2: Equivalent corrugation profile.

$$\epsilon = \frac{\sigma}{E} = \frac{278}{56,000} \approx 0.005 \frac{\text{in.}}{\text{in.}}$$

that is,  $\epsilon = 0.5$  percent @  $\Delta y = 0.125$  inch, which is probably a low enough level of strain for linear deflection. Thus, again the actual test data and theoretical determination are in reasonably good agreement.

**Summary of Example 2.**—The overall comparison of the actual test results by the parallel-plate, load-deflection method, and the analyses or theoretical predictions, are within about 10 percent of the same value for the various performance parameters—such as, tube strength-deflection ratio  $\left(\frac{W}{\Delta y}\right)$ , tube unit weight ( $w$ ), and maximum tube deflection for linear stress/strain ( $\sigma/\epsilon$ ) in the tube wall plastic material. Thus, the analytical procedure outlined in this report is considered adequate for the structural design of corrugated plastic drainage tubing.

### APPENDIX III

Major equations and definitions of terms are expressed in metric units. Only the more important general equations are included here; formulae used to derive these general equations are not presented. The same equation numbers that are used in the report are used here also, but are shown as primed numbers.

$$\Delta y = 0.1488 \frac{\left(\frac{D_{NA}}{2}\right)^3}{EI} (W) \quad [1']$$

$$\Delta x = 0.1366 \frac{\left(\frac{D_{NA}}{2}\right)^3}{EI} (W) \quad [2']$$

where,

$\Delta y$  change in vertical tube diameter, (cm.);

$\Delta x$  change in horizontal tube diameter, (cm.);

$D_{NA}$  diameter of tube to the neutral axis (NA) of the tube-wall cross section, (cm.);

$E\Delta$  modulus of elasticity (Young's Modulus) for tube-wall material, (g./cm.<sup>2</sup>);

$I\Delta$  moment-of-inertia of the tube-wall cross section, (cm.<sup>4</sup>/cm. tube length);

$W\Delta$  parallel-plate load applied, (g./cm. tube length); 0.1488 and 0.1366 are dimensionless constants related to angular position around the circumference;

$2$  = the dimensionless ratio between the tube diameter and radius.

$$W_c = C_c w_s B_c^2 \quad [3']$$

where,

$W_c\Delta$  total soil load on conduit, (g./cm. tube length);

$C_c\Delta$  load concentration factor related to  $\left(\frac{H_s}{B_c}\right)$  ratio and soil type, where  $H_s$  = drain depth, (cm.) (This factor can be determined graphically from (12));

$w_s\Delta$  unit weight of soil, (g./cm.<sup>3</sup>);

$B_c\Delta$  outside diameter of drain tube, (cm.).

$$\Delta x_s = \frac{D_i K_S W_c \left(\frac{D_{NA}}{2}\right)^3}{EI + 0.061 E' \left(\frac{D_{NA}}{2}\right)^3} \quad [4']$$

where,

$\Delta x_s\Delta$  change in horizontal diameter of drain tube under soil loading (cm.);

$D_L\Delta$  deflection lag factor (generally between 1.0 and 1.5);

$K_S\Delta$  bedding factor constant related to conduit bedding angle  $2\alpha$  (see fig. 2, p. 5);

$E'\Delta$  soil modulus term, (g./cm.<sup>2</sup>) [see fig. 2];

0.061 = a dimensionless constant,

and,

$W_c$ ,  $D_{NA}$ ,  $E$ , and  $I$  as defined previously.

$$I = \frac{1}{12P} [2T_w H^3 + L_i T_i^3 + L_o T_o^3 + 3H^2(L_i T_i + L_o T_o)] \quad [10']$$

where,

$P\Delta$  corrugation pitch, (cm.);

$T_i\Delta$  thickness of tube wall at the inside diameter, (cm.);

$T_o\Delta$  thickness of tube wall at the outside diameter, (cm.);

$T_w\Delta$  thickness of tube wall webs, (cm.);

$L_i\Delta$  length of corrugation root at inside diameter, (cm.);

$L_o\Delta$  length of corrugation ridge at outside diameter, (cm.);

$H\Delta$  effective structural depth of corrugations, (cm.); and,

$I$ , as defined previously.

$$D_{NA} = D_i + H + T_i \quad [21']$$

where,

$D_i\Delta$  inside diameter (ID) of drain tube (cm.); and,

$D_{NA}$ ,  $H$ , and  $T_i$  as defined previously.

$$A_w = \frac{1}{P} (L_o T_o + L_i T_i + 2T_w H) \quad [25']$$

where,

$A_w\Delta$  cross-sectional area of tubing's corrugated wall per unit length of tube (one side only) (cm.<sup>2</sup>/cm. tube length); and,

$P$ ,  $L_o$ ,  $T_o$ ,  $L_i$ ,  $T_i$ ,  $T_w$ , and  $H$  as defined previously.

$$w = \pi D_{NA} A_w \rho_p \gamma_{H_2O} \quad [29']$$

where,

$\pi$  = Constant, 3.1416 (dimensionless);

$w\Delta$  Tubing unit weight, (g./cm. tube length);

$\rho_p\Delta$  Specific gravity of plastic material (dimensionless);

$\gamma_{H_2O}\Delta$  density of water, (g./cm.<sup>3</sup>); and,

$D_{NA}$  and  $A_w$  as defined previously.

$$\sigma_c = \frac{W_c}{2A_w} \quad [31']$$

where,

$\sigma_c\Delta$  "Pure" ring compression stress in the tube wall (g./cm.<sup>2</sup>);

and,

$W_c$  and  $A_w$  as defined previously.

$$\sigma_B = 2.66 \left[ \frac{EH + \left(\frac{T_o}{c}\right)}{D_{NA}^2} \right] (\Delta x) \quad [38']$$



where,

$\sigma_B \triangleq$  bending stress in the tube wall, (g./cm.<sup>2</sup>)

2.66 = dimensionless constant

and,

$E, H, T_o, c, D_{NA}$ , and  $\Delta x$  as defined previously.

$$\sigma_{TC} = \sigma_c + \sigma_{BC} \quad [41']$$

where,

$\sigma_{TC} \triangleq$  maximum total tube wall compressive stress (g./cm.<sup>2</sup>);

$\sigma_{BC} \triangleq$  compressive component of tube wall bending stress (g./cm.<sup>2</sup>);

and,

$\sigma_c$  as defined previously.

**END**